Development of novel measurement methods and radiation hard particle sensors for timing applications

Thesis topic defence seminar

Iskra Velkovska

Advisor: Prof. Dr. Marko Mikuž

Co-advisor: Dr. Bojan Hiti

May 14, 2024

Outline

- Introduction to HL-LHC and ATLAS experiment
- Plan for PhD research
- Introduction to Silicon particle sensors
- ATLAS HGTD irradiation tests
- Novel LGAD sensors for improved radiation hardness and fill factor
- 3D timing detectors
- New experimental methods for characterization of radiation defects
- Summary

LHC and ATLAS experiment

- Large Hadron Collider (LHC):
  - sits in a tunnel 100 m underground, 27 km circumference at CERN near Geneva, Switzerland
  - Proton-proton collisions up to $\sqrt{s} = 13\ TeV$
- Bunch structure of proton beam:
  - Bunch crossing every 25 ns
  - ~10^{11} protons in each bunch
  - Pile-up -> challenge for HL-LHC
    - increase from current μ=30 up to μ=200
- Upgrade starts 2026, first collisions 2029
  - Instantaneous luminosities up to L ≃ 7.5×10^{34} cm^{-2} s^{-1} (currently ~ 2x10^{34})

- ATLAS (A Toroidal LHC ApparatuS) particle detector consists of:
  - Inner Tracker: detects paths of charged particles
  - Calorimeter: measures energy of electrons/photons/hadrons
  - Muon Spectrometer: tracks muons
  - Magnet Systems: superconducting toroid magnets->bend the paths of charged particles

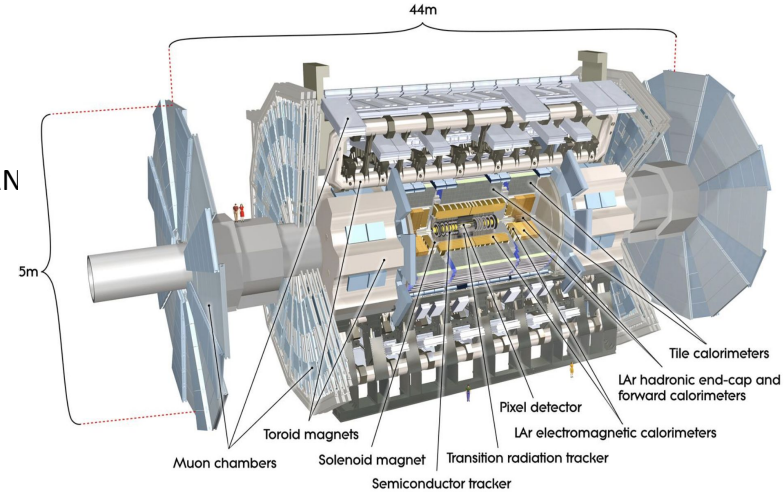

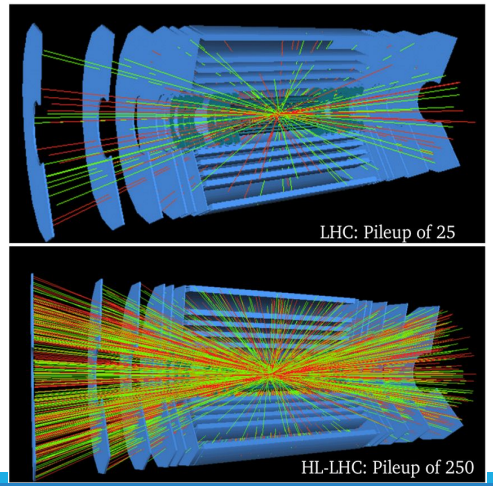

Timing detectors at HL-LHC

- Vertices distributed (Gaussian) with: σ_z=5 cm & σ_t=180 ps
- Tracking detectors provide resolution of primary vertices in forward region typically >1 mm, which leads to merging of several collision vertices

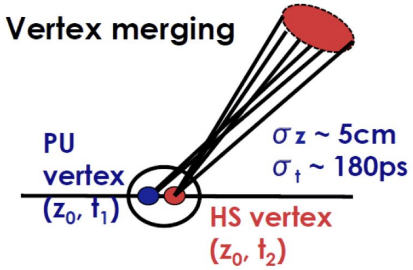

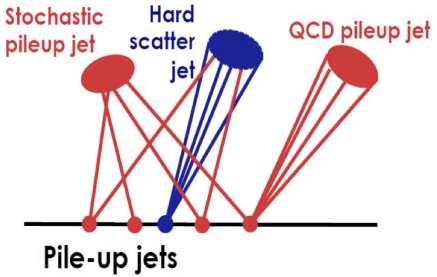

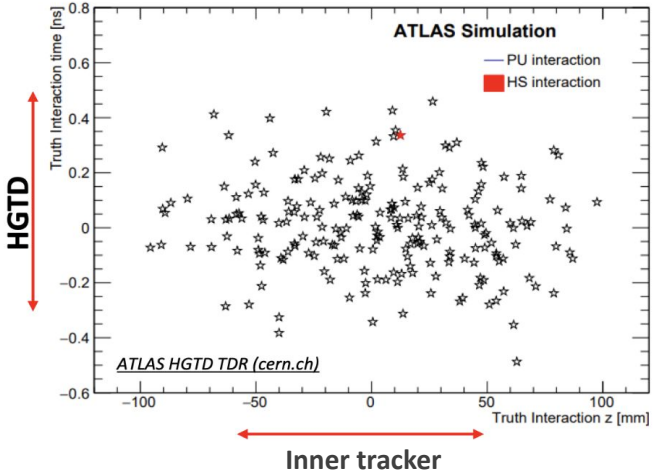

PU->Pile-up jet->arises from pile-up collisions
HS->Hard Scatter jet->carry information such as momentum and energy

- The High Granularity Timing Detector (HGTD) will provide track timing resolution of around of <50 ps for minimum ionizing particles (MIP)
- Distinguish between hard scatter jets and pile-up jets by providing precise timing information about time-of-arrival (ToA) of particles

➢ improves track-to-vertex association in the forward region
➢ spatial and temporal resolution of particle interactions

ATLAS: High Granularity Timing Detector

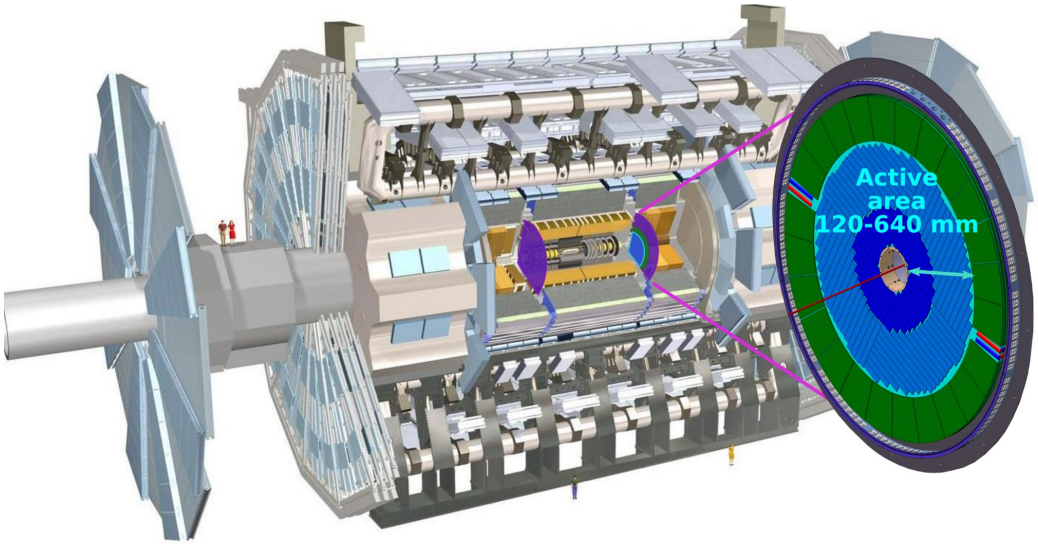

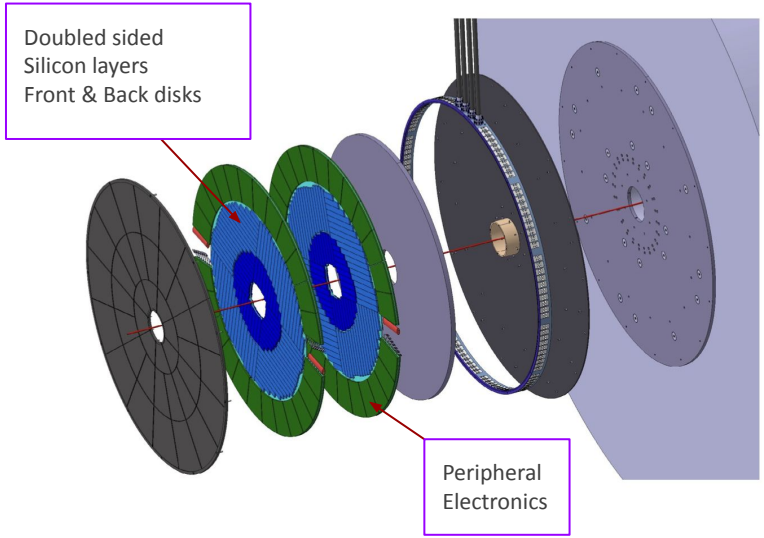

- Located between barrel and end cap calorimeters (|z|=3.5 m)
- Two instrumented double-sided layers
- provides timing information to tracks in the region of 2.4<|η|<4.0
- Design based on 1.3 × 1.3 mm^2 silicon pixels
- 3.6 million channels operating at -30^oC (6.4 m^2 of Si)
- Radiation damage up to 5.1 x 10^{15} n_{eq} /cm^2 and 4.7 MGy
- integrated luminosity of 4000 fb^{-1}

Plan for the PhD research

- In my thesis I will investigate novel sensors and measurement techniques for detecting particles in high energy physics experiments with emphasis on precise time measurements
- Irradiation testing of sensors produced for ATLAS HGTD (ongoing)
- Research and characterization of LGAD sensor designs for improving radiation hardness/fill factor
- Investigate properties of 3D silicon detectors for timing applications
- Investigate new experimental techniques for characterization of radiation defects

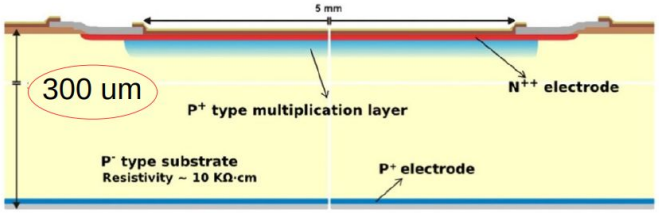

E. Cavallaro et al., NIM A 796 (2015) 136

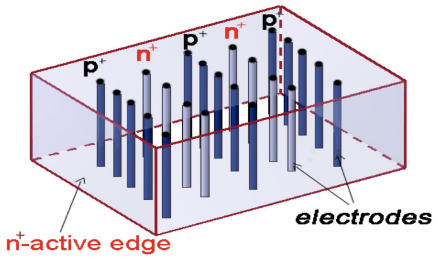

Introduction to Silicon sensors

- Minimum Ionizing Particle (MIP) passes through a silicon sensor under reverse bias
  - produces electron-hole pairs, generating a measurable current pulse
- Reverse bias voltage means applying a voltage with p-side of the silicon connected to the negative terminal of a power supply, and n-side to positive terminal
  - creates a depletion region near the p-n junction

- Depletion of sensor is needed for:
  - charge collection efficiency
  - improved signal-to-noise ratio
  - spatial resolution
  - radiation hardness

Leakage current *I (T)* -> thermal generation of e-h pairs *(uA/cm²)*

$$I(T) \propto T^2 \exp\left(\frac{E_{ef}}{2k_B T}\right)$$

The width of the depletion zone *w* is given by:

$$w = \sqrt{\frac{2\epsilon\epsilon_{\mathrm{Si}} V_{\mathrm{bi}}}{e_0 N_{\mathrm{eff}}}}$$

$N_{eff} = N_D - N_A$ is the **effective doping concentration**, i.e. the difference between the ionized donor and acceptor concentration

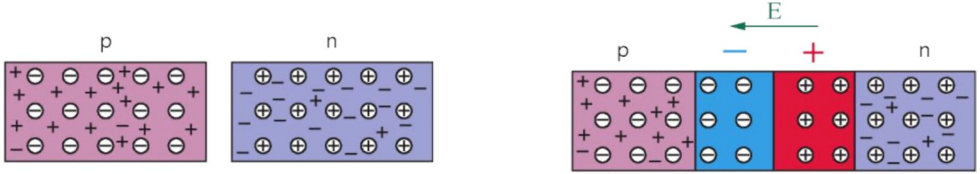

Formation of P-N junction, *Doctoral thesis, Electric field and charge multiplication in radiation-damaged silicon detectors, Marko Milovanovic, 2016*

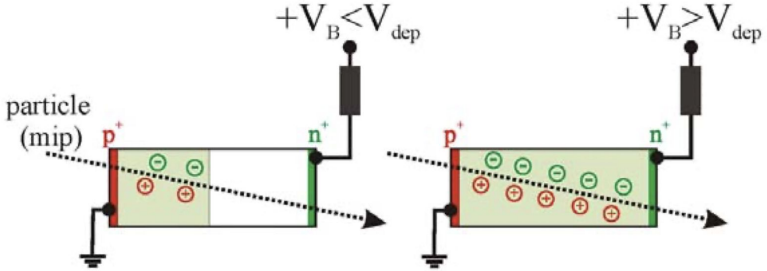

Minimum Ionizing Particle (MIP) -> charged particle which transverses material

Signal formation

- In presence of external applied electric field, signal inside silicon bulk is induced by mov charges (electrons/holes), drifting with velocities $\boldsymbol{v}_{dr}(\boldsymbol{E}(\boldsymbol{r}(t)))$
- Induced charge-> signal in sensors can be calculated by **Shockley–Ramo**'s theorem
  - Signal current induced in the sensing electrode by a point charge is given by:

$$I = q\vec{v}\vec{E}_w \text{ for particle track } Q(t) = \sum_{e-h} \int_{t=0}^{t_{int}} I_{e,h} dt$$

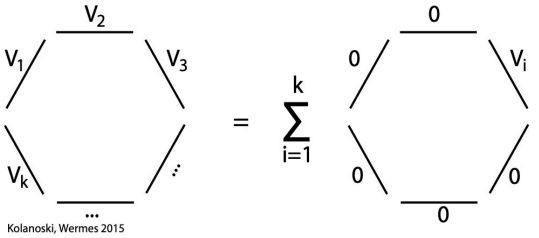

Illustration of a system of k electrodes

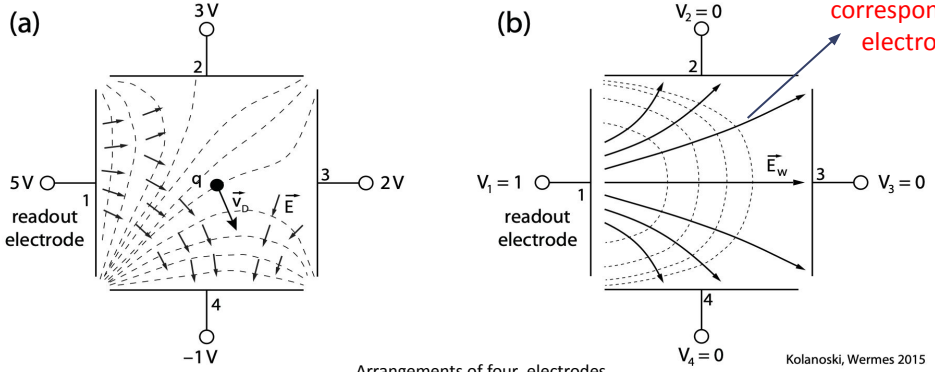

Arrangements of four electrodes

Citation: Particle Detectors- Fundamentals and applications, Hermann Kolanoski and Norbert Wermes

- The method relies on calculation of the weighting field $\boldsymbol{E}_W$
  - describes electrostatic coupling between charge at given point in the detector and its electrodes

$$dQ_i = -q\,\vec{E}_{w,i}\,d\vec{r},$$

$$i_{S,i} = q\,\vec{E}_{w,i}\,\vec{v}_D\,.$$

Time resolution in silicon detectors

$$\sigma_t^2 = \sigma^2_{tw} + \sigma^2_{jitter} + \sigma^2_{TDC}$$

σ^2_{tw} correctable (amplitude variations) and uncorrectable (Landau)

σ^2_{jitter}-variations due to noise in the signal (electronic jitter)

σ^2_{TDC}- contribution from the time-to-digital-converter binning of the readout electronics

- Good time resolution demands thin sensors
- Capacitance can be reduced by making the pixels small
- Large pad dimensions >> thickness required to mitigate weighting field effect

➔ Presence of capacitance-related noise can degrade the signal-to-noise ratio (SNR) of the sensor's output signal

➔ higher capacitance values-> higher equivalent resistances-> increased thermal noise

Jitter component

$$\sigma_j = \frac{\sigma_n}{\left|\frac{dV}{dt}\right|} \approx \frac{\sigma_n}{\left|\frac{S}{\tau_p}\right|} = \frac{\tau_p}{S/N}$$

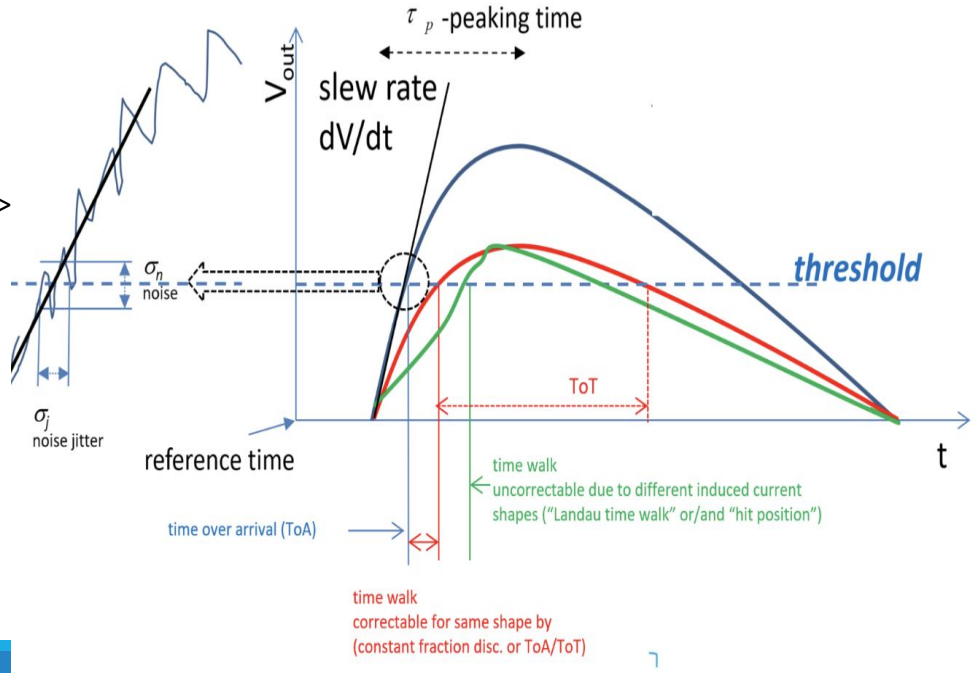

HGTD sensors: Low Gain Avalanche Detectors (LGADs)

- Excellent time resolution requires high S/N ratio -> charge multiplication integrated into sensor ->LGADs
- n-on-p silicon sensor with additional p+ Gain Layer
- Charge multiplication by impact ionization ⟶ improved S/N

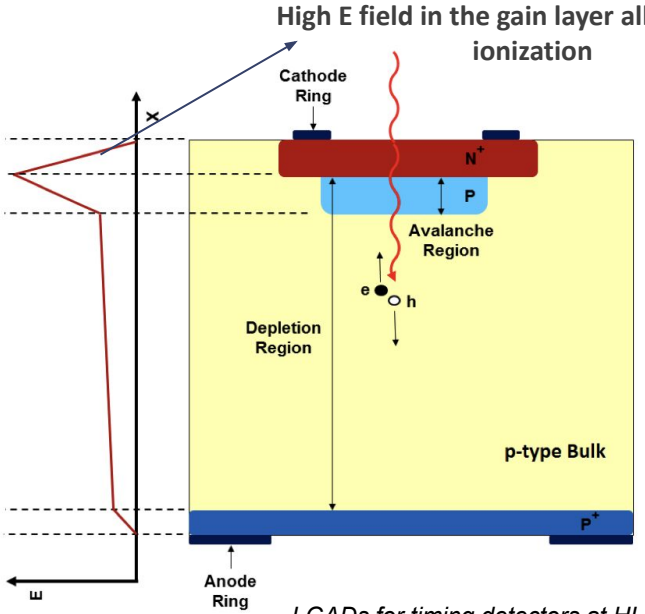

LGADs for timing detectors at HL-LHC, Gregor Kramberger

- optimized for fast timing response and enhanced radiation tolerance
- Active sensor thickness 50 um, physical thickness of silicon 300 um
- Thinner detector-> smaller Landau fluctuations-->low signal

- High field region is implemented in a silicon sensor by doping
- Electrons will produce an avalanche in this high field region
- Impurities added to reduce the changes of gain layer doping after irradiation

In LGAD gain layer depletion voltage is calculated as:

$$V_{gl} = \frac{N_{eff} d^2 e_0}{2\varepsilon_r \varepsilon_0}$$

where ***d*** is the thickness of the gain layer

Radiation damage in silicon detectors

- Bulk damage (NIEL->Non-Ionizing Energy Loss), creation of silicon lattice defects (fluence)
  - Increase of leakage current
  - Changes in effective doping concentration critical in LGADs because it degrades gain layer via acceptor removal
  - Trapping of the drifting charge
- Surface damage, oxide charge buildup and appearance of interface traps
  - Increase of surface current
  - Modification of electric field underneath the oxide
  - Trapping near the surface
- Variation of current (ΔI) with fluence (Φ_{eq}) expressed through α as current related damage factor :

$$\alpha = \frac{\Delta I}{V \cdot \Phi_{eq}}$$

Impinging particle hits the lattice atom and knocks it out of the lattice site:

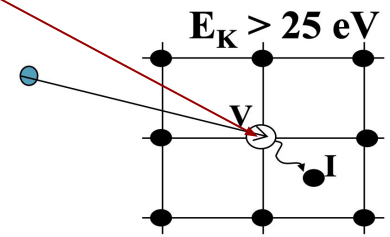

point defects: Frekel pair
(Vacancy–Interstitial pair)

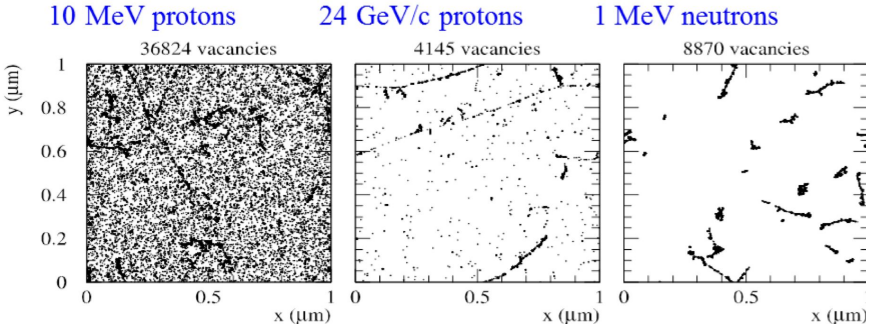

Different particles can create different damage at the same NIEL

ATLAS HGTD Irradiation Tests

ATLAS HGTD sensor production

- over 16,000 sensors required for ATLAS-HGTD
- 8-inch wafers with 52 Main Sensors
- 15 x 15 pixel sensors (2 x 2 cm)
- Two sensor designs selected for HGTD: IHEP (Beijing, China) and USTC (Hefei, China), both produced by IME
- Quality Control Test Structure (QCTS) next to each Main Sensor

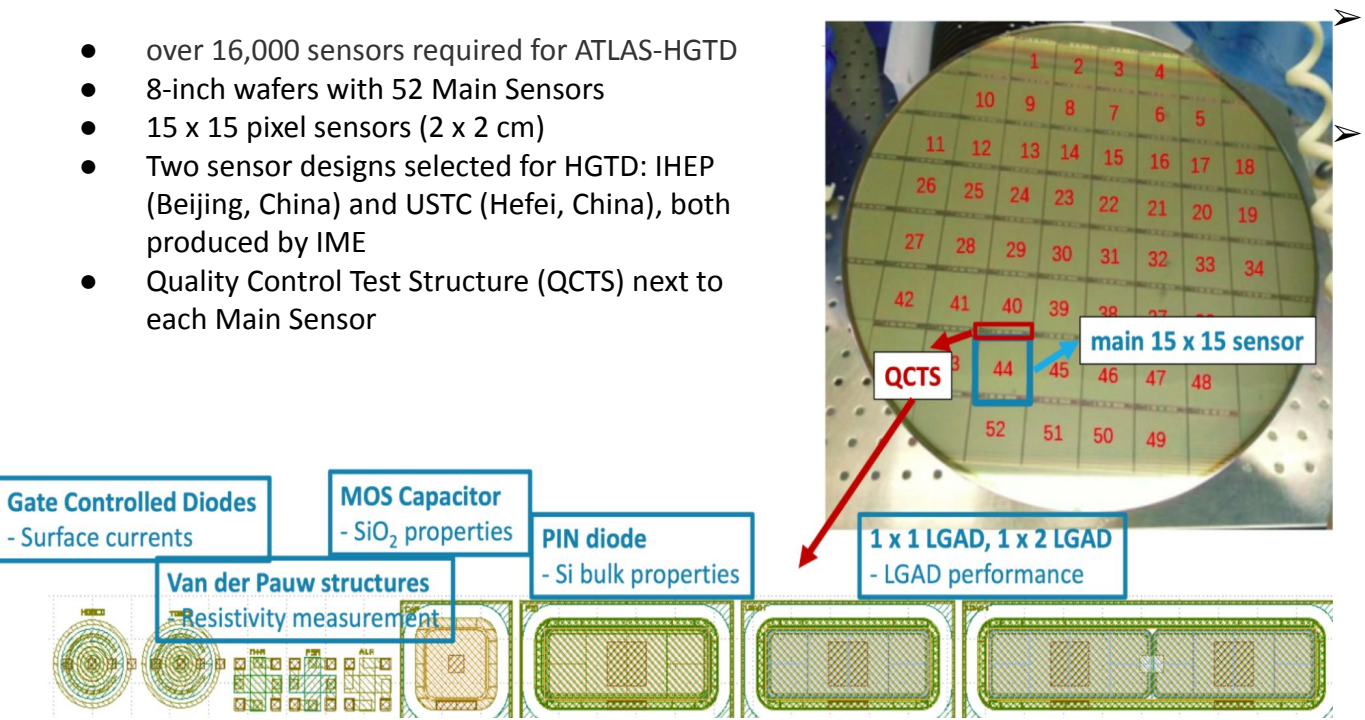

Irradiation tests (IT) to monitor sensor radiation hardness throughout ATLAS production
Main test site is JSI Ljubljana – neutron irradiation (TRIGA reactor) and tests on QCTS

- New Transient Current Technique (TCT) test method
- TCT-IT not directly measuring MIP charge and time resolution – calibration by timing β-Sr90 measurements
- Comparaison with CV (Capacitance-Voltage) - IV (Current-Voltage) measurements- Process Quality Check

HGTD Radiation hardness requirements: >= 4 fC Collected charge and < 50 ps time resolution at 550 V bias at End of Life (EOL) fluence of 2.5 x 10^{15} n_{eq}/cm^2

Irradiation Tests with Transient Current Technique

- Characterization of each wafer (lots of measurements ~1000) so we need fast method-> method based on TCT
- TCT setup with focused infrared light-> penetrates deep in semiconductor, reduced scattering
- Test method: scanning TCT between two LGADs on QC-TS
- Extracted Parameters: gain layer depletion voltage->V_{gl} , bulk depletion voltage-> V_{fd} , Gain, leakage current-> I_{leak}
- Calibrated with other methods: ^{90}Sr timing/collected charge

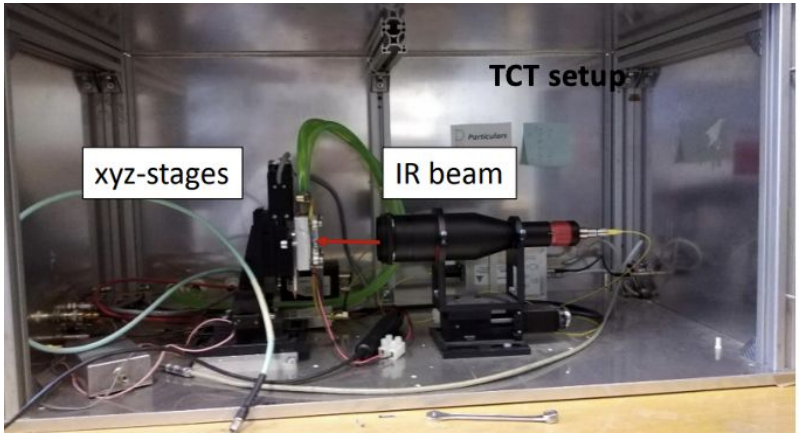

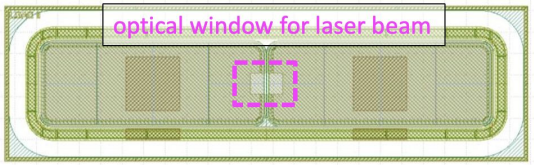

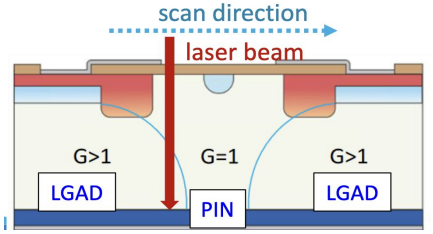

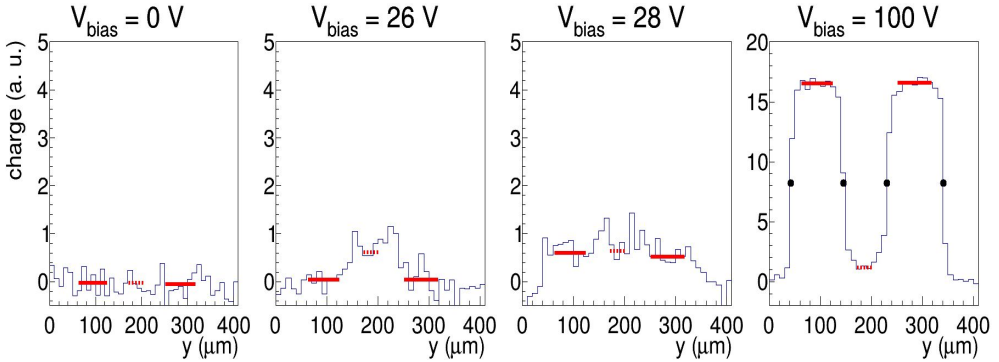

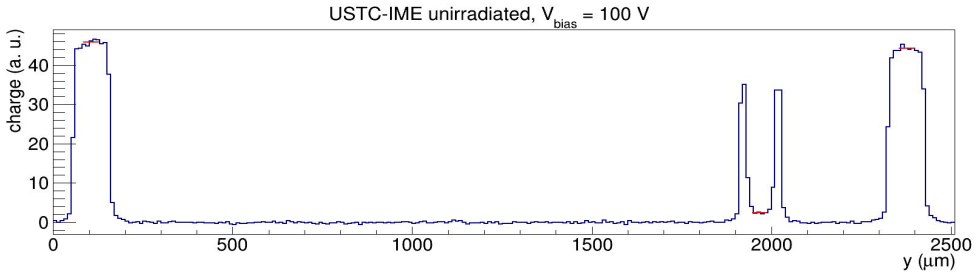

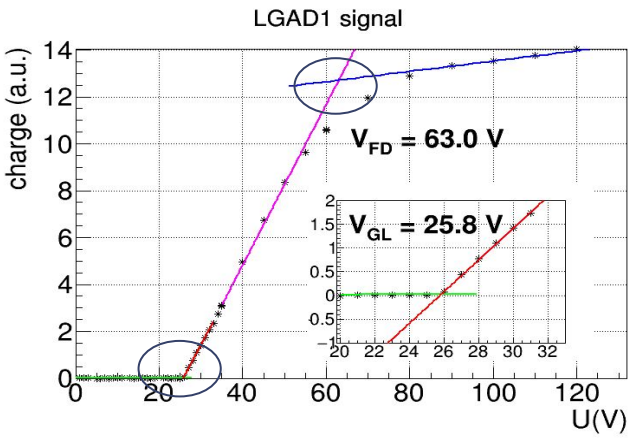

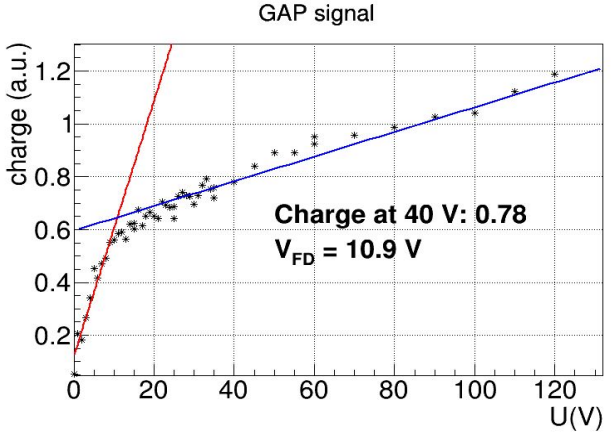

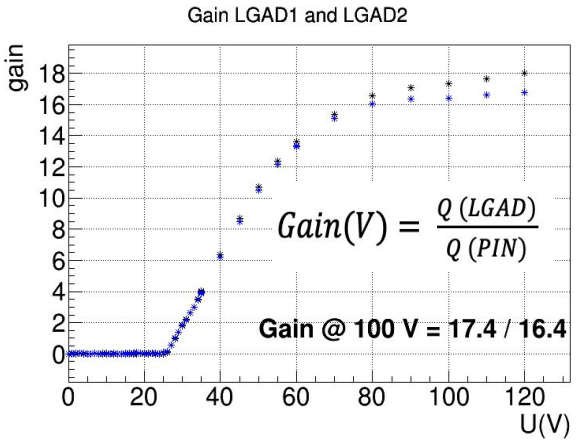

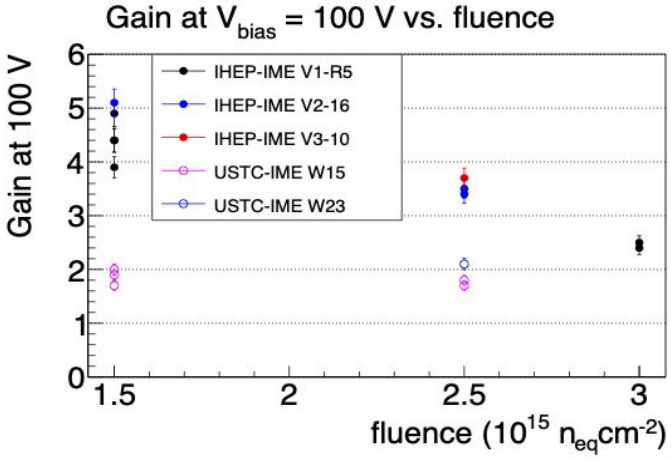

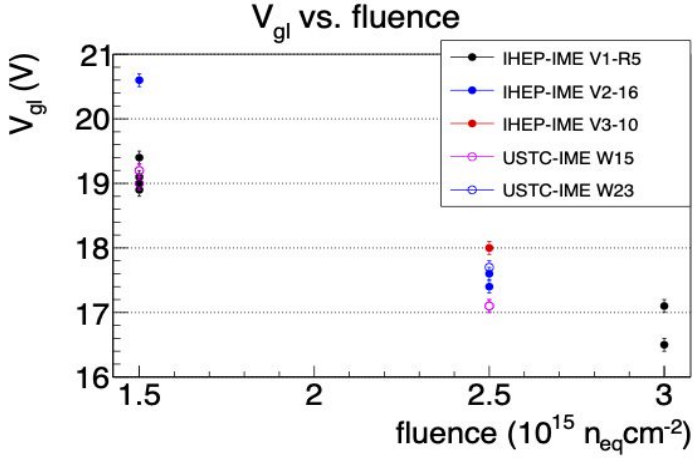

- ***V_{gl}*** ->falling consistently with fluence
- ***Gain***-> falling consistently with fluence (due to smaller V_{gl})

β-^{90}Sr Timing/Collected charge Irradiation tests

- TCT-IT not directly measuring **MIP charge** and **time resolution**
  - Sr90 is a pure β emitter – laboratory MIP source
- Setup with two LGADs (time reference and Device Under Test (DUT))
- DUT cooled to -30 °C
- Coincidence trigger on PMT + reference LGAD -> DUT doesn't take part in trigger!
- Measurement of charge and time resolution as function of voltage
- lots of measurements are being done for the TCT calibration->Sr90 will be phased out

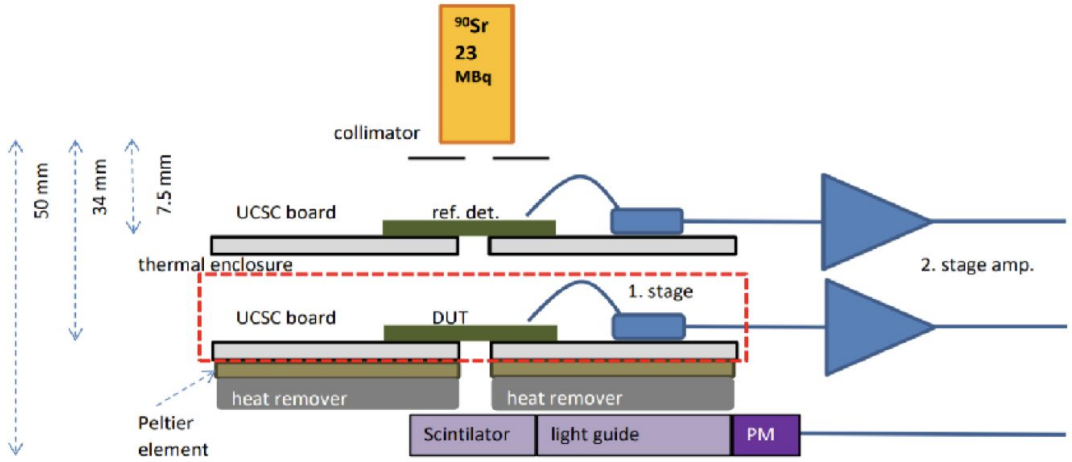

Sr90 results: charge and time resolution

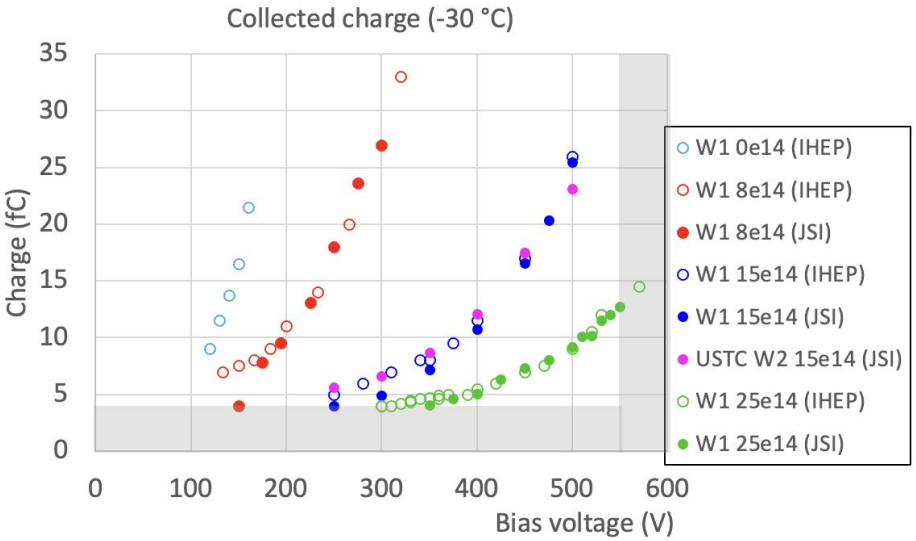

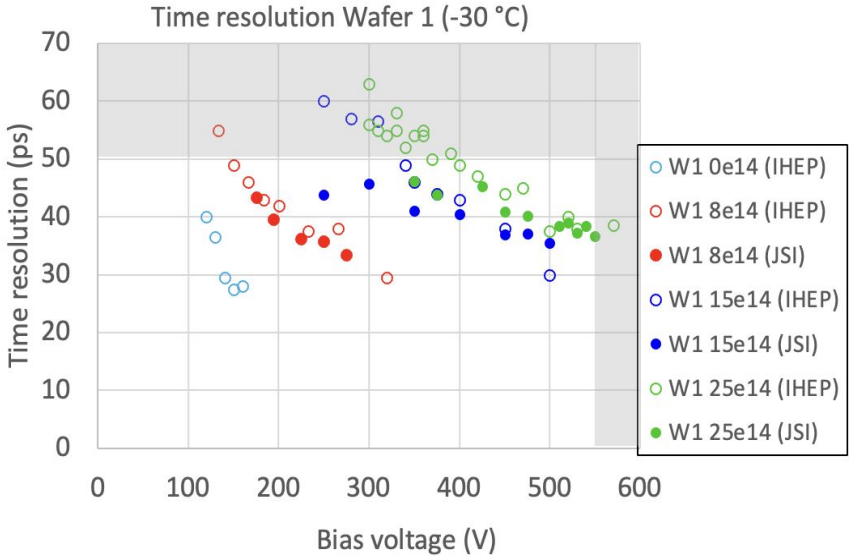

- ➔ Collected charge and time resolution degrade with fluence
- ➔ Results still well within HGTD specifications
- ➔ Excellent agreement in values between different sites (method is reliable)

Acceptance/Rejection criteria for wafers

Sensors after 2.5e15 (End of Life fluence) need to fulfill:

- Collected charge 4 fC (Most Probable Value – MPV) at 550 V
- MIP time resolution < 50 ps

- Correlation of Vgl measured in TCT and Sr90 MIP charge
  - Acceptance Criteria
    - set at V_{gl} -> charge below threshold ~5 fC
    - set at Gain -> charge below threshold
  - more measurements will be done with wafers that fail the first test

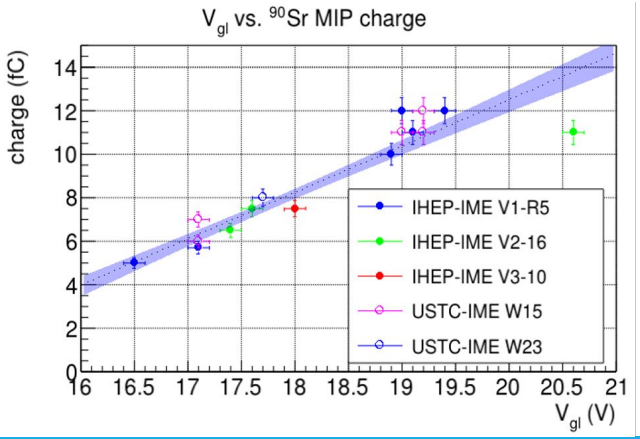

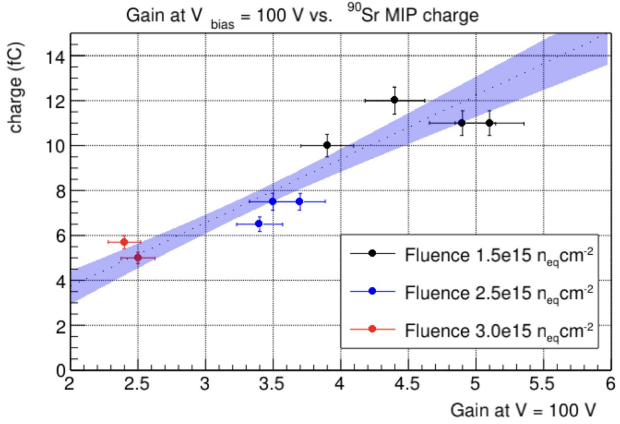

Novel timing sensor designs

Radiation hardness
Reducing of acceptor removal

Fill Factor
100 % efficiency (geometric)

Partially activated boron

Compensated LGADs

Trench isolated LGADs

Inverse LGADs

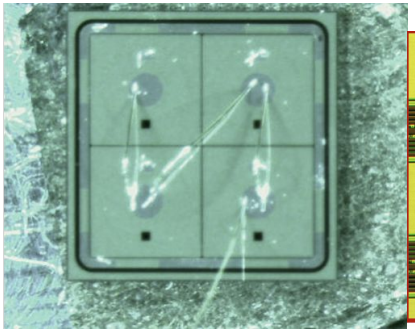

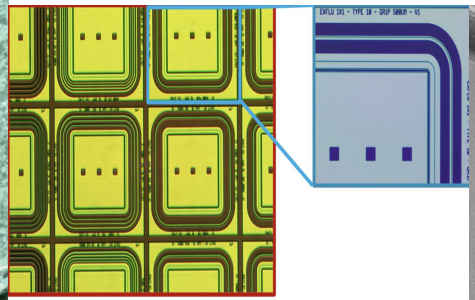

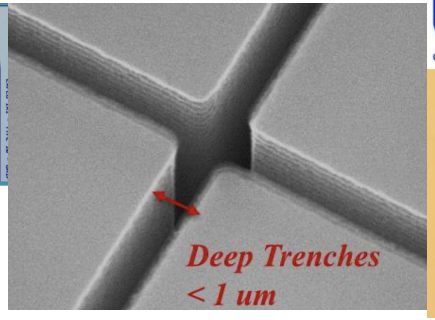

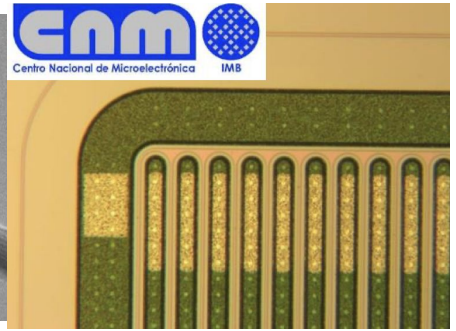

HPK LGADs with Partially Activated Boron research

- Study on the importance of radiation hard LGADs
- HPK has produced a Half Activated Boron (HAB) run of LGAD devices
- Part of boron implanted, but not electrically activated in the gain layer
- Radiation hardness improvement-> results from inactive boron shielding the electrically active boron, hence reducing acceptor removal

→ 2x2 LGAD array
→ 1.3x1.3 mm^2
→ 50 um thickness

- Three sample flavours were characterized at JSI:
  - **Reference** (full boron activation)
  - **0.5 HAB** (same activated boron concentration as reference + non activated boron 0.5x reference)
  - **1 HAB** (same activated boron as reference + non activated boron 1x reference)

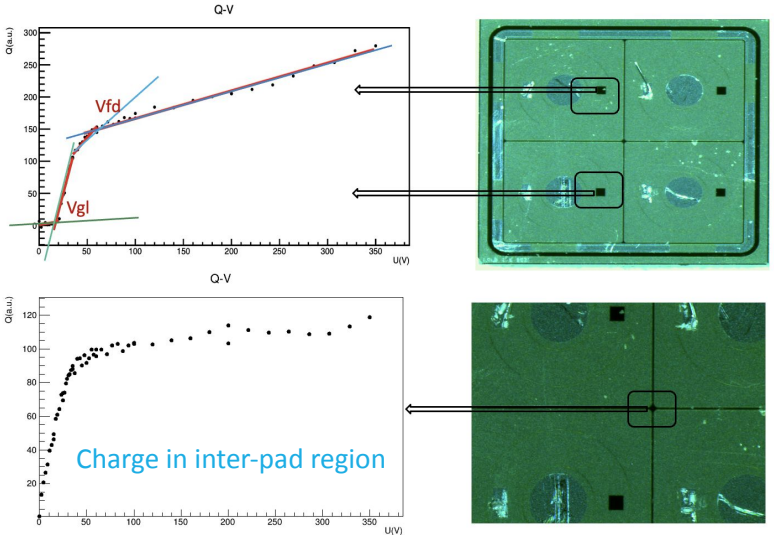

Conclusion: Small effect of HAB on acceptor removal

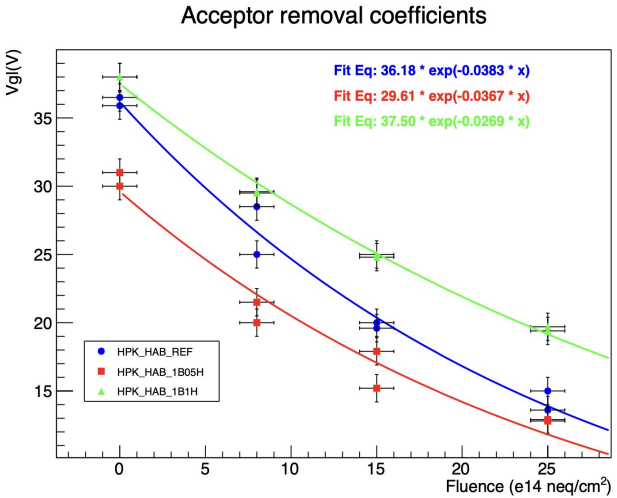

Acceptor removal coefficients
c (REF)= 3.8e-16 cm^2
c (1B05H)= 3.4e-16 cm^2
c (1B1H)= 2.6e-16 cm^2

Timing ^{90}Sr results for HPK samples

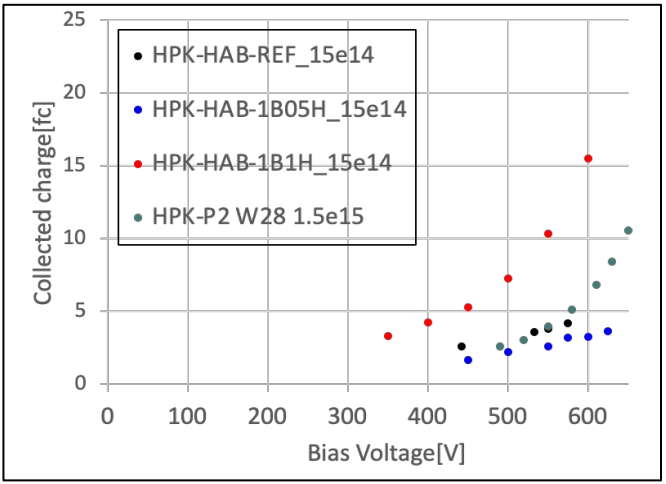

- 2x2 HPK LGADs were irradiated to fluence of 15e14 n_{eq}/cm^2
- Comparison with HPK-P2 (ATLAS/CMS prototype run from 2020)
- Due to highest doping before irradiation the best performance after 15e14 cm^{-2} is measured for 1B1H sample

- Only marginal gain up to 350 V for irradiated samples showing not sufficient radiation hardness

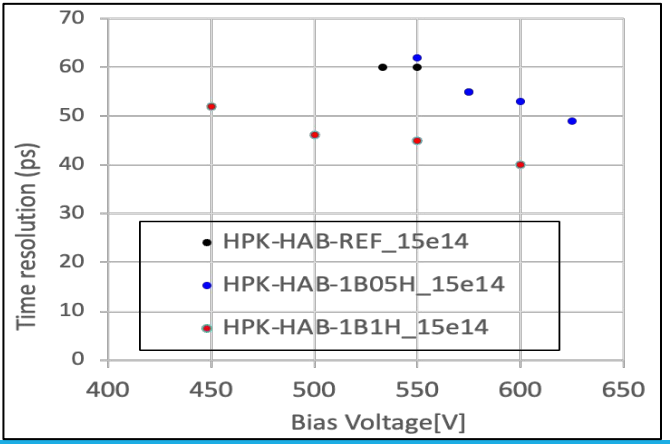

Preliminary version of paper has been written!

- after 15e14 cm^{-2} achievable time resolution just below 50 ps
- significant degradation of collected charge after irradiation
- Radiation hardness below state-of-the-art level required for ATLAS-HGTD

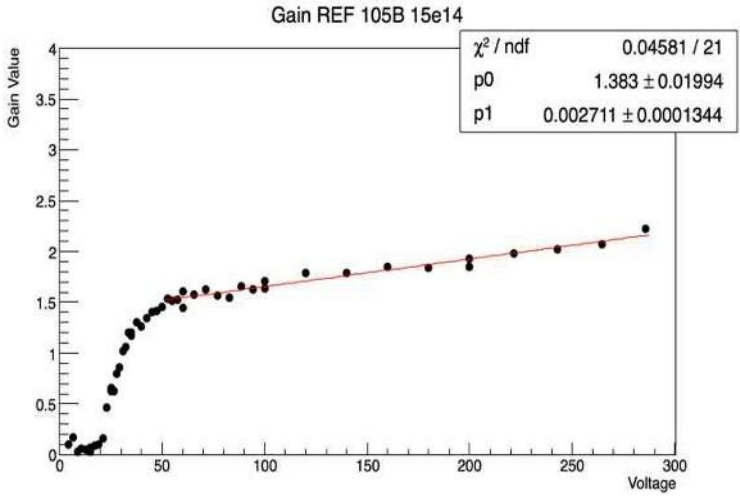

Compensated LGADs

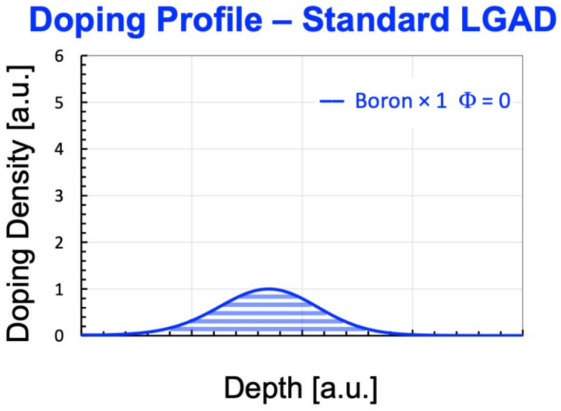

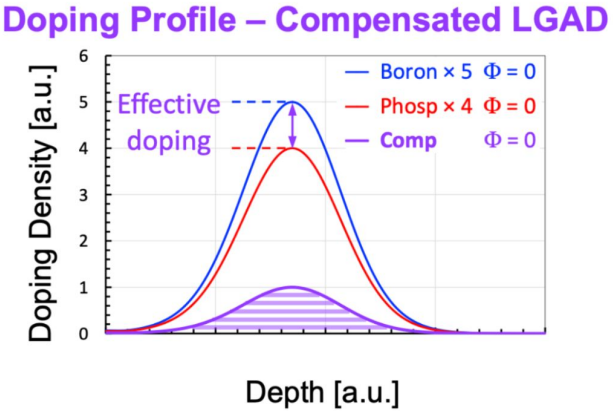

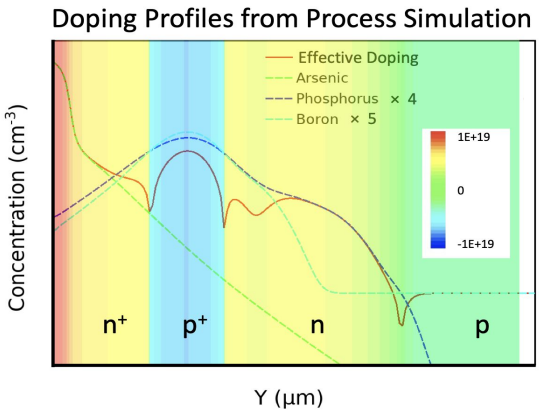

Characterisation of the first compensated LGADs from FBK before and after irradiation, Valentina Sola et al., 2023

- ➔ gain layer results from the overlap of a p+ and an n+ implant
- ➔ difference between acceptor and donor doping will bring effective concentration similar to standard LGADs
- ➔ both acceptor and donor atoms will undergo removal with irradiation
- ➔ production of samples ongoing as part of RD50 project
- ➔ characterization of these samples will be done in the scope of the thesis

Fill factor solutions- TI-LGAD, iLGAD

TI-LGAD technology:

Goal: Sensor with small pixels (~100×100 um or smaller) and high fill factor (95 % or higher)

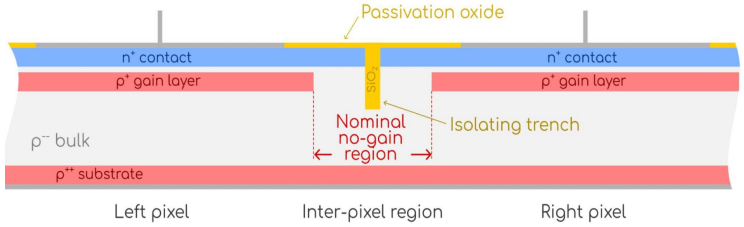

- Fill factor quantifies the efficiency of the LGAD in utilizing its surface area for sensing purposes
- higher fill factor indicates a greater proportion of the surface area dedicated to active sensing
- crucial to maximize its detection efficiency and precision in timing measurements for HGTD

iLGAD: a p-in-p micro-strips

- no segmentation in the multiplication layer
- collects positive carriers (h)
- complex double side process

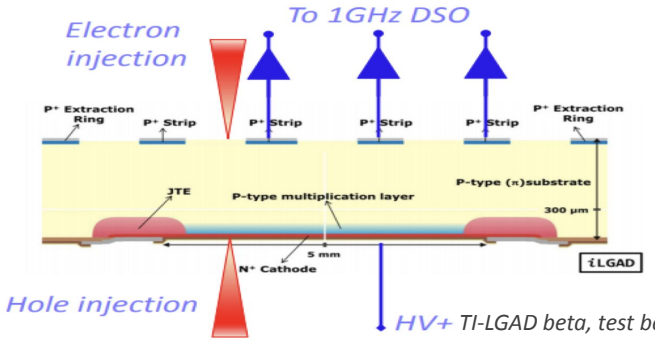

Charge sharing in TI-LGADs

(testbeam analysis)

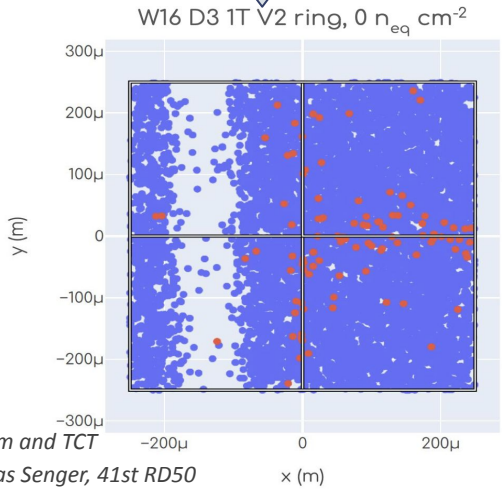

TI-LGAD beta, test beam and TCT characterization, Matias Senger, 41st RD50 Workshop, Sevilla (2022)

3D timing detectors

- vertical columns of electrodes that penetrate the bulk detector
- Size of (50 × 50) μm^2 and thickness of 285 µm

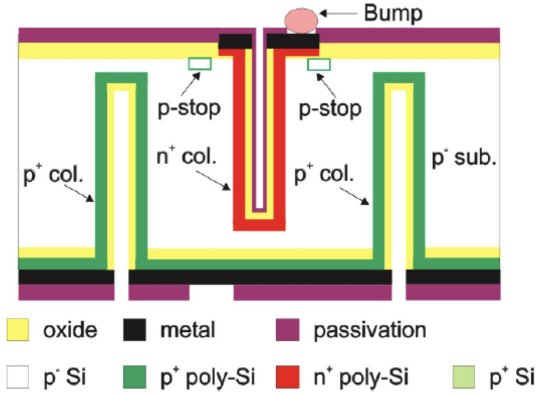

LGAD and 3D as timing detectors, The 28th International Workshop on Vertex Detectors, (2020)

- ➢ short interelectrode distance-> capability to withstand high amounts of radiation (at low V_{bias})
- ➢ very short charge travel time-> **candidates for timing detectors**
- ➢ already have 3D sensor prototypes produced by CNM Barcelona in the scope of CERN-RD50 project

- ➢ leakage current of 20-40uA with a breakdown voltage below 40 V before irradiation
- ➢ @150 V time resolution is ~30 ps @-30 ℃

- ➢ Characterization of charge collection and time resolution in 3D detectors as part of the thesis with test beam and lab techniques
- ➢ Comparison with simulations

ADVANTAGES:

- **low depletion voltage**
- **short charge collection distance**
- **less trapping probability after irradiation**
- **lower charge sharing**

DISADVANTAGES:

- non uniform spatial response (electrodes and low field regions)
- complicated technology (cost, yield)
- higher capacitance with respect to planar

Simulations for 3D detectors

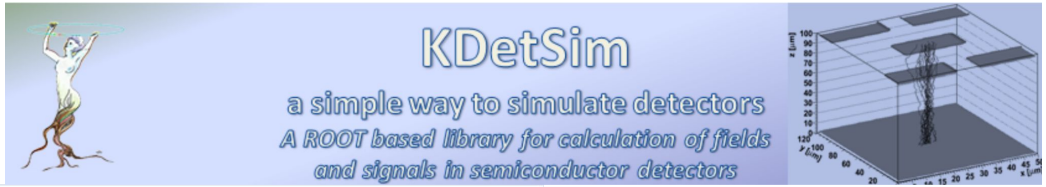

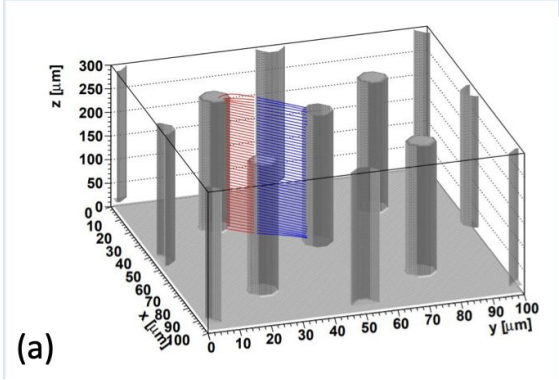

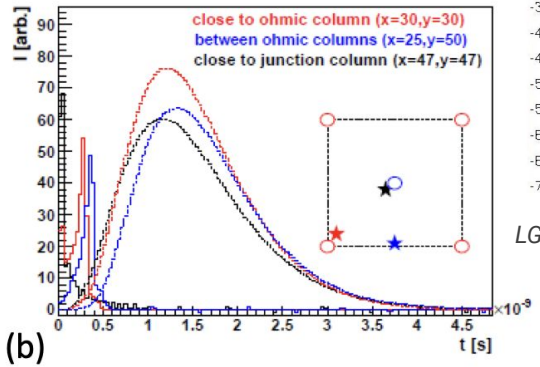

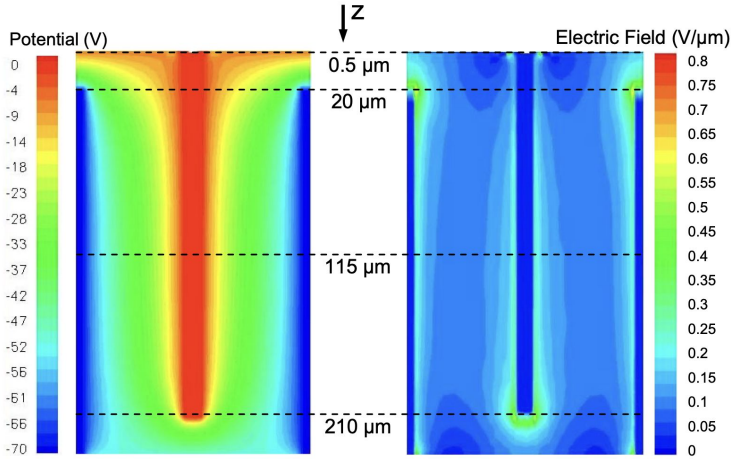

LGAD and 3D as timing detectors, The 28th International Workshop on Vertex Detectors, (2020), Test beam measurements of CNM 3D pixel detectors, G. Pellegrini. 20th RD50 Workshop, Bari

(a) Simulation of the paths of the electrons (blue) and holes (red) created by the perpendicular track of a MIP (minimum ionizing particle)

(b) Simulation of the waveform induced with different hit positions before (solid lines) and after (dashed) the electronics response

- The response of a 3D pixel silicon sensor when being hit by a MIP can be simulated by using the software KDetSim

Introduction to testbeam

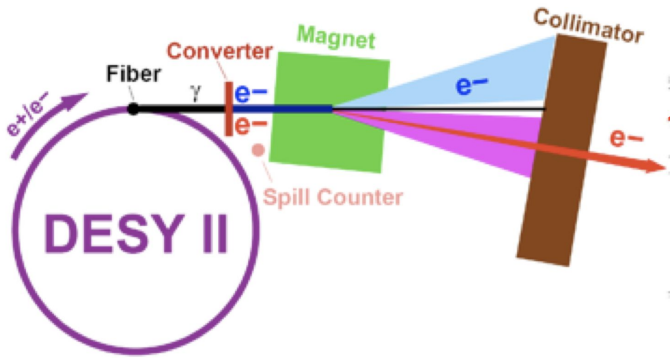

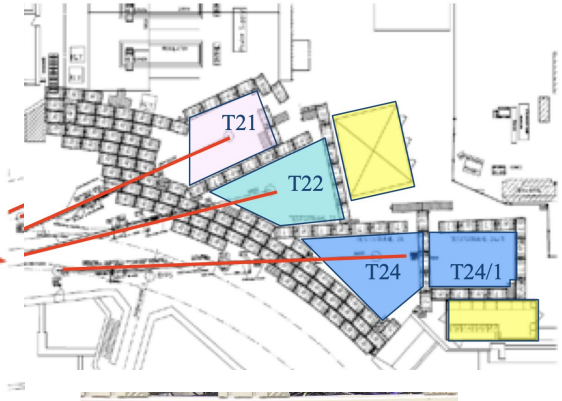

DESY Bremsstrahlungs/conversion beam with electron energy up to 6 GeV.

EUDET beam telescope

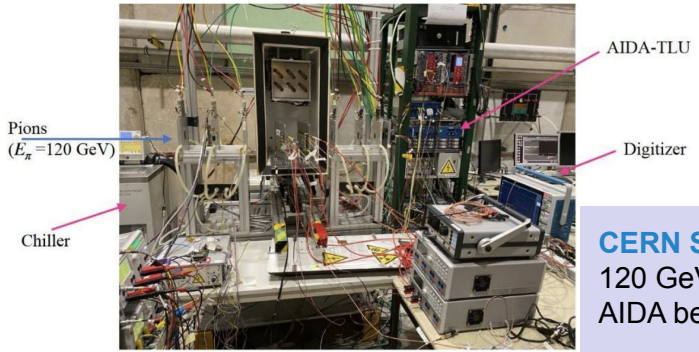

Timepix3 telescope

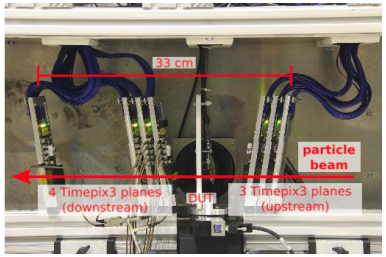

CERN SPS
120 GeV pion beam
AIDA beam telescope

What is a beam telescope?

A tool to define the exact track of a particle in a test beam very precisely. Used for detailed studies of newly developed detectors.

Testbeam analysis

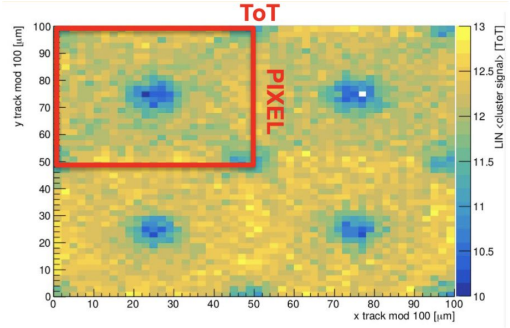

Cassese, A., Trento Workshop, 2020

- For testbeam data is used **Corryvreckan->** software for reconstruction and analysis

Corryvreckan
The Maelstrom for Your Test Beam Data

- The pixel hit information comprises:
  - Pixel address (column and row)
  - Pixel timestamp: time-of-arrival (ToA)
  - Pixel charge: time-over-threshold (ToT)
- Charge can "leak" from one pixel into neighbouring cells by lateral diffusion. This effect is called **charge sharing**.
  - As a consequence, a clustering algorithm is needed to group such pixels into one cluster
- For the tracking, clusters within a certain spatial and time interval on the planes of the reference telescope are combined into a straight-line track-> DUT plane excluded

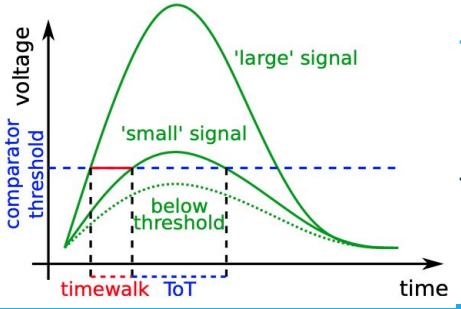

time-over-threshold (ToT) and the effect of **timewalk** for pulses

measured resolution

$$\sigma_{\text{measured}} = \sqrt{\sigma^2_{\text{telescope}} + \sigma^2_{\text{DUT}}}$$

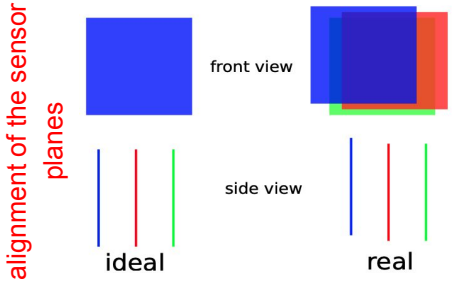

Development of TCT technique for characterization of radiation damage

- will try to develop new methods to assess radiation damage
- DC laser will populate trap levels and the pulse will be used to measure sensor response
- Pulsed laser to probe signal dependence on trap occupation

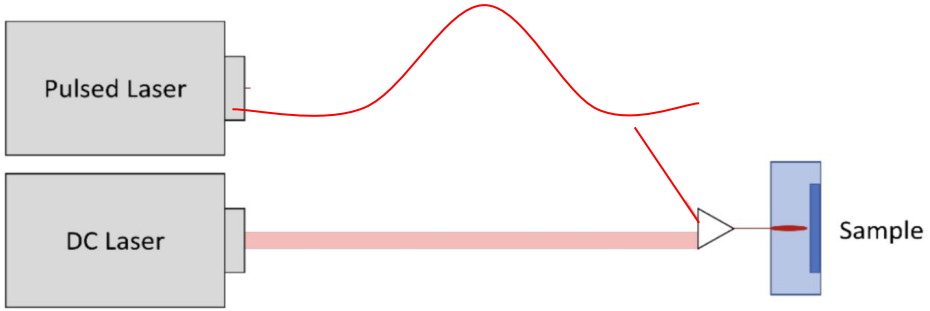

- Research on how different DC levels populate the trapping centers and how this reflects on the signal shape/size
- This is a new technique and its measurement power will be tested

Summary

- In this thesis novel sensors and new measuring techniques for detecting particles in high energy physics experiments with emphasis on precise time measurements will be studied
- Irradiation testing of sensors produced for ATLAS HGTD (ongoing) with:
  - Transient Current Technique (TCT) and ^{90}Sr timing/collected charge measurements
- Understanding new LGAD sensor designs for improving radiation hardness/fill factor
- Properties of 3D silicon detectors for timing applications will be investigated
- New experimental techniques for characterization of radiation defects

Thank you for the attention!

BACKUP

CV-IV results: Acceptor removal parameter

- Comparison of TCT results with CV-IV probe station measurements
- Measured test structures: LGADs at fluences $0e^{14}$, $8e^{14}$, $15e^{14}$, $25e^{14}$ n_{eq}/cm^2

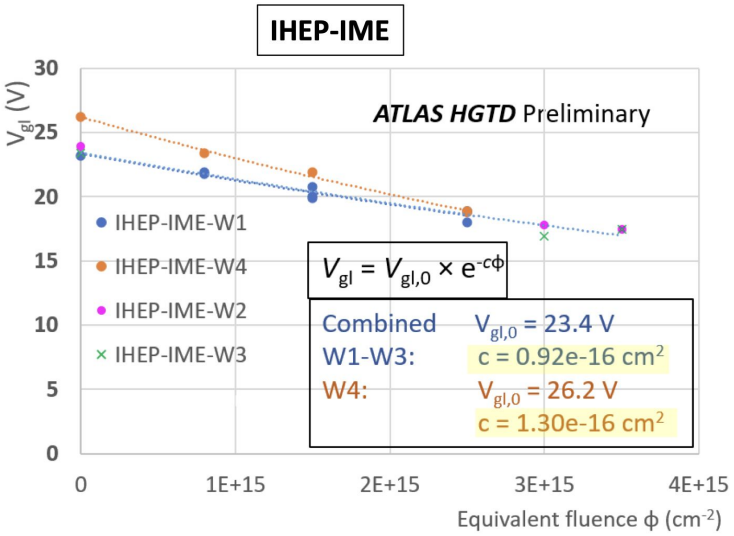

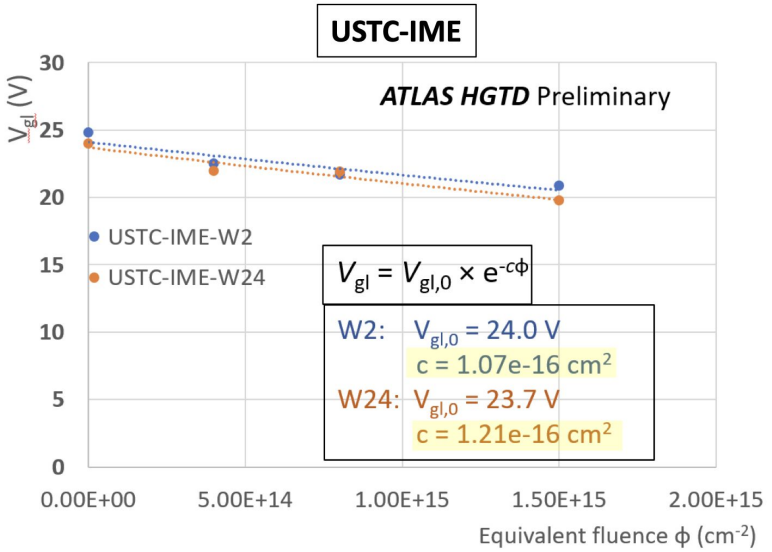

- CV: Acceptor removal parameter c in all IHEP-IME and USTC-IME wafers is around $1e^{-16}$ cm^{-2} (slight differences)
- Promising result in terms of acceptor removal → indicates good radiation hardness

Effective acceptor removal

- Acceptor-> atom that can accept an electron-> creates hole
- Substituting silicon atoms-> Boron, Carbon, Aluminium
- Gain of the LGADs depends on the doping of the gain layer -> doping of the gain layer is affected by radiation, due to the process called "acceptor removal"

R. Wunstorf et al, NIMA 377 (1996) 228.)
J. Adey, PhD Thesis, Univeristy of Exceter, 2004
J. Adey et al., Physica B 340–342 (2003) 505–508

Acceptor removal

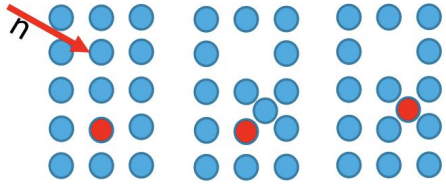

G. KRAMBERGER, LGADS FOR TIMING DETECTORS AT HL-LHC, CERN DETECTOR SEMINAR, 2021

- Different ways to mitigate acceptor removal:
  - Dope gain layer with carbon – approach for ATLAS HGTD and CMS ETL
  - Narrow B implantation
  - Partial activation of boron (HAB)

$$dN_B = -\sum_i c_i \cdot N_B d\Phi \quad , \quad c = \sum_i c_i\,([O],[C],[B])$$

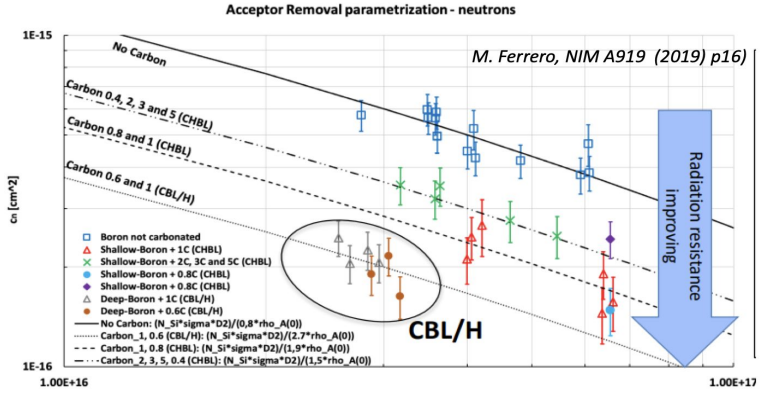

Dependence of the acceptor removal vs. fluence Φ:

$$V_{GL}(\Phi) = V_{GL}(0)*e^{(-c*\Phi)}$$

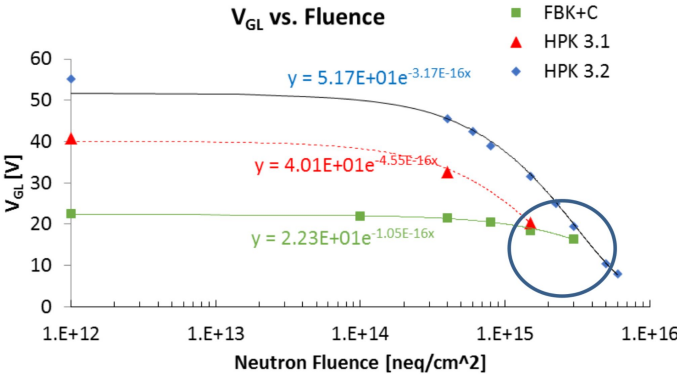

Shockley–Ramo's theorem

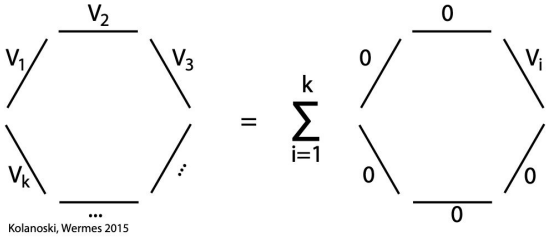

Fig. 5.3 Schematic illustration of a system with k electrodes lying on respective potentials V_i $(i = 1, \ldots, k)$. This system can be represented by a sum of k arrangements, each one with another electrode on its actual potential and all others grounded.

$$\phi_0(\vec{r}) = \sum_{i=1}^{k} \phi_i(\vec{r}), \qquad \text{with} \qquad \begin{matrix} \phi_i|_{S_i} = V_i, \\ \phi_i|_{S_j} = 0, \quad j \neq i. \end{matrix}$$

We consider an arrangement of k electrodes to which voltages $V_1, V_2, \ldots, V_k$ are applied. Thanks to the superposition principle the potential generated by the electrodes $\varphi_0(\vec{r})$ in the space between the electrodes can be represented by a sum over different configurations of potentials φ_i (i = 1,...,k). For each configuration i all electrodes remain at a potential 0 except for the potential of the electrode i which lies on its actual voltage V_i (fig. 5.3):

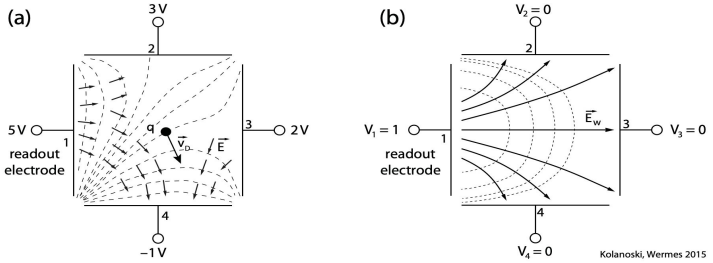

Fig. 5.4 Example of an arrangement of four electrodes. (a) Actual field and potential configuration and the resulting direction of motion of a charge; (b) Configuration for the computation of the weighting field corresponding to electrode 1. Field profiles are depicted by arrows and potential contours by dashed lines.

The Shockley–Ramo theorem [889,805] states that the signal induced by a moving charge q on an electrode i is given by the weighting potential or the weighting field of the potential configuration $\varphi_i(\vec{r})$:

$$dQ_i = -q\,\vec{E}_{w,i}\,d\vec{r},$$

$$i_{S,i} = q\,\vec{E}_{w,i}\,\vec{v}_D\,.$$

TCT measurement method

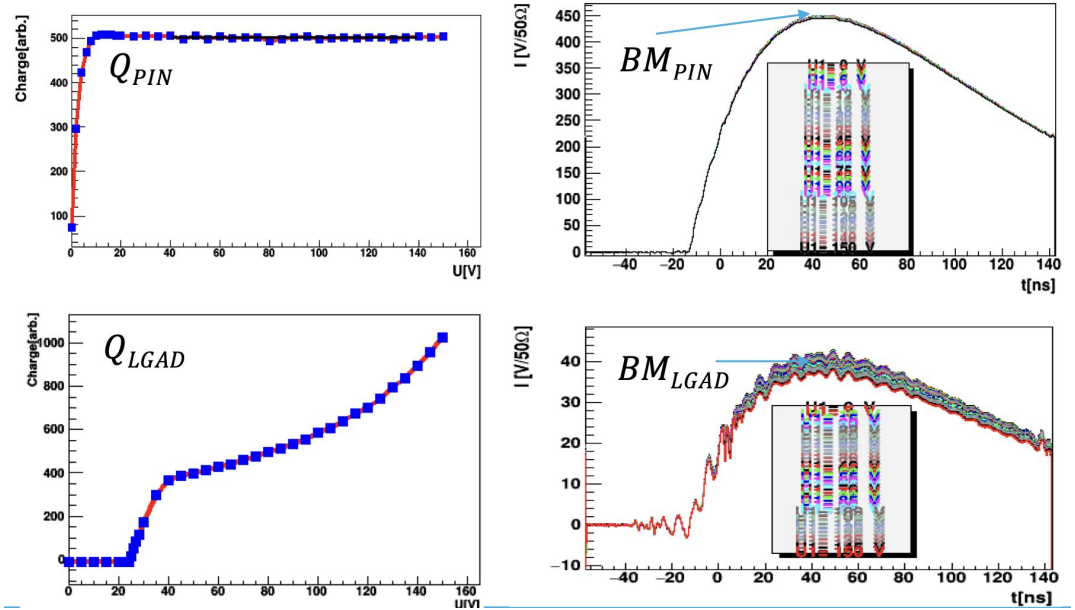

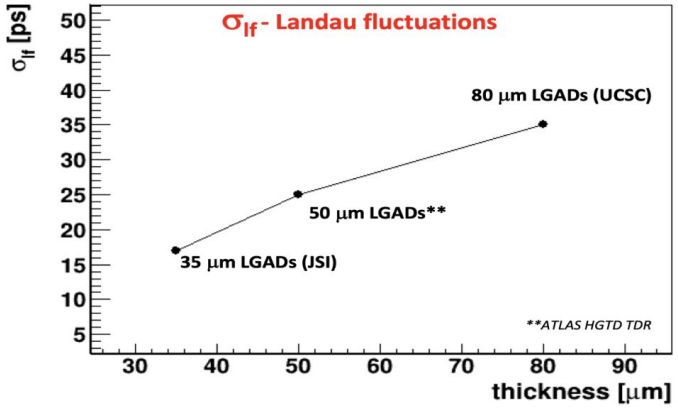

- Signal from PIN – average over the 100 V above the full depletion voltage
- Signal from LGAD – taken at every voltage point above the full depletion voltage
- Peaks of the BM output for both LGAD and PIN

Silicon Detectors after Irradiation

Irradiation degrades the signal of silicon detectors

Recovers by increasing bias voltage

Charge multiplication by impact ionization-due to very strong electric field

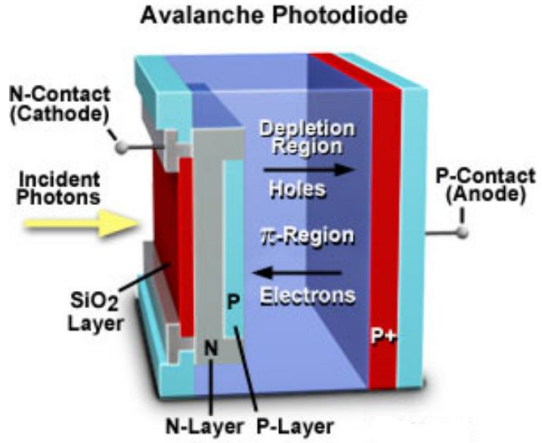

Devices with charge multiplication:

- Avalanche Photodiodes (APDs)
- Photodiodes (Gain=1)
- Geiger mode (SPAD/SiPM)Gain~1E7

Avalanche diodes are similar in design to the silicon ***p-i-n*** diode.

Depletion layer in an avalanche photodiode is relatively thin, resulting in a very steep localized electrical field across the narrow junction.

LGAD Performance: Time Resolution

Ultimate tests of LGADs in beam tests

- Timing performance extracted from Δt(LGAD-ref) distributions
- Achieved ~60ps resolution after 1E15neq/cm2

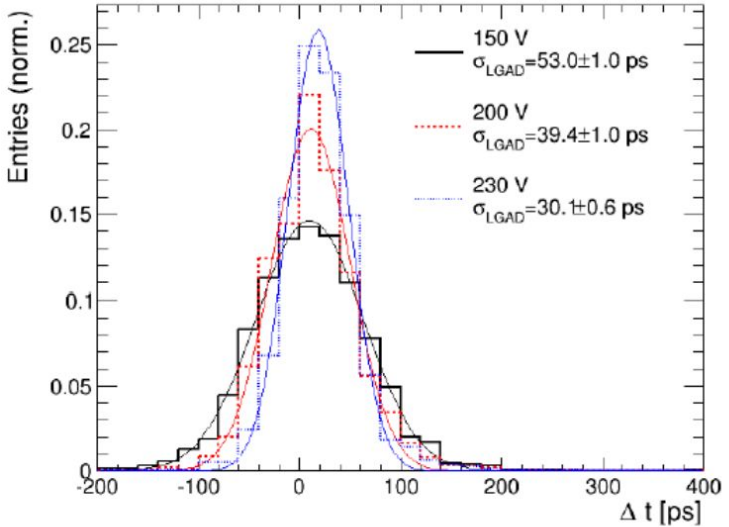

ATLAS HGTD

Time resolution of silicon sensors

Silicon radiation detector technologies

- based on reverse biased p-n junctions
- impinging radiation creates electron–hole pairs when passing through Si detector
- In presence of an electric field, these charge carriers drift toward electrodes, inducing current signal- fed to an external amplifier

- operated in full depletion conditions- for optimal efficiency, high signal-to-noise ratio, short time response
- radiation hardness for HEP: damage to Si lattice due to high fluences

Operation principle of a silicon radiation detector

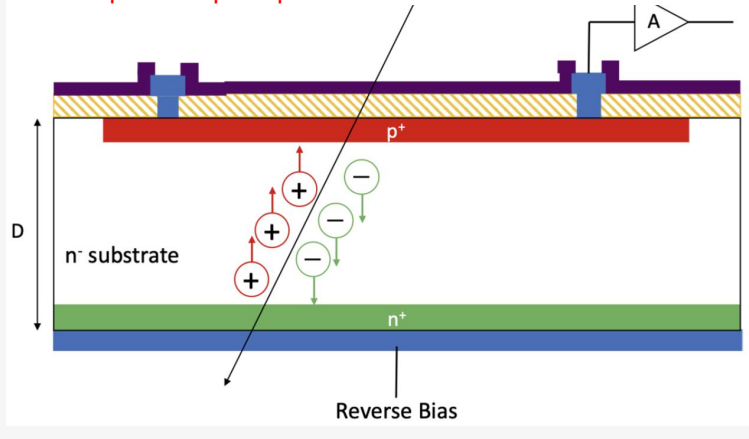

TCT

IHEP-IME_UBM_V4_16_04_0e14

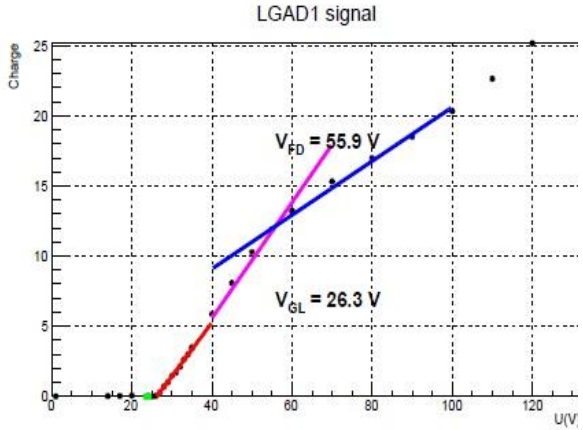

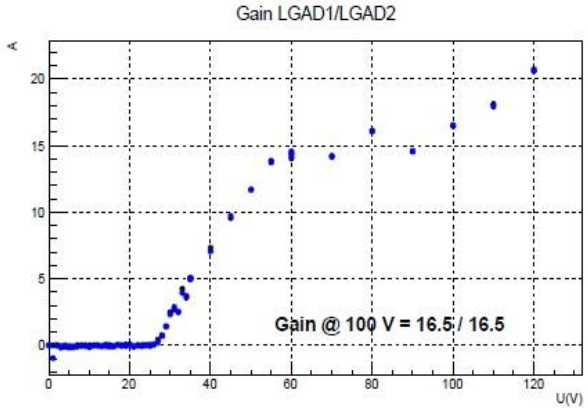

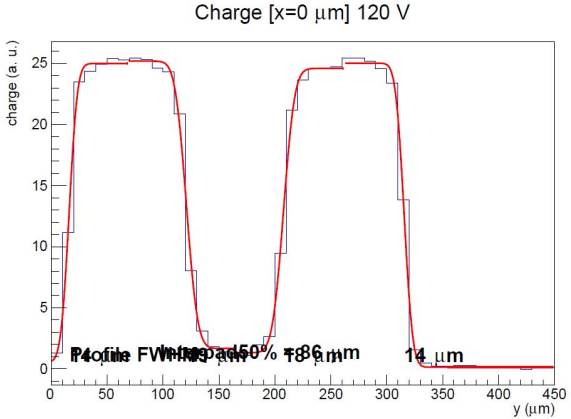

IHEP-IME_UBM_V4_10_04_0e14

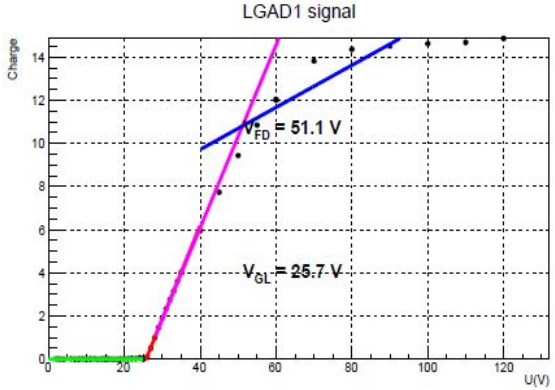

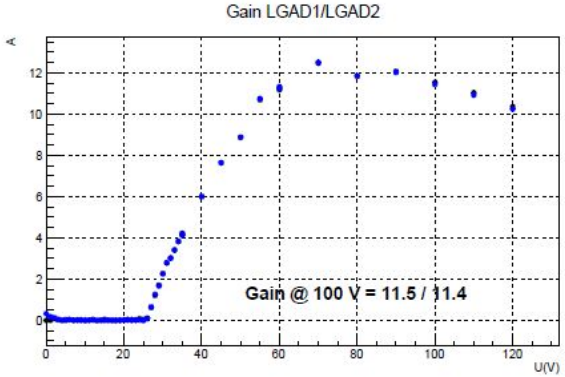

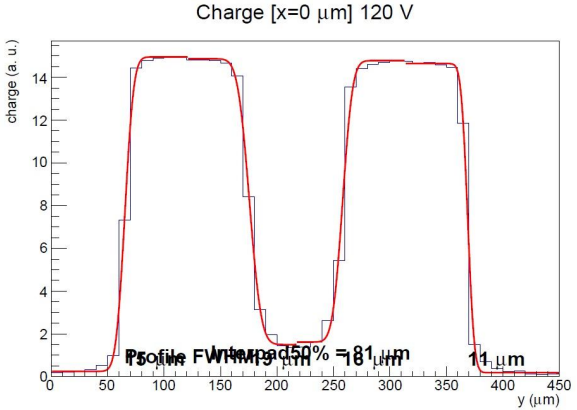

HGTD Irradiation tests ^{90}Sr results- temperature dependence

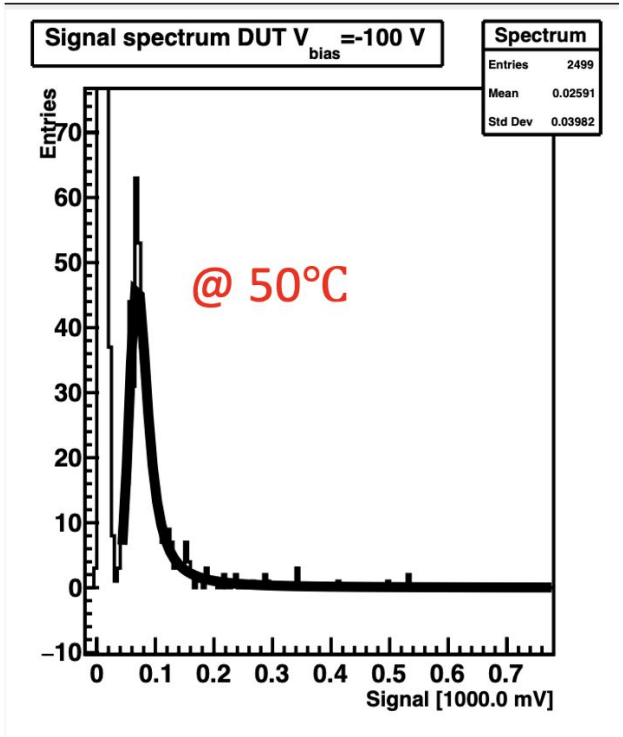

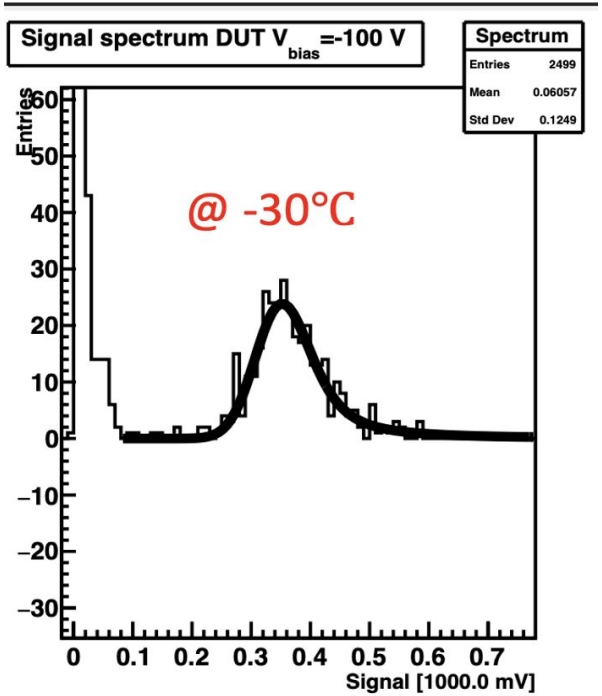

➢High temperature decreases gain
➢Shift in the signal spectrum
➢Gain is dependent on Impact Ionisation rate proportional to the temperature

Timing Sr90 results- IHEP-IME and USTC-IME samples UBM-ed @-30 °C, fluence: 0e14 neq/cm^2

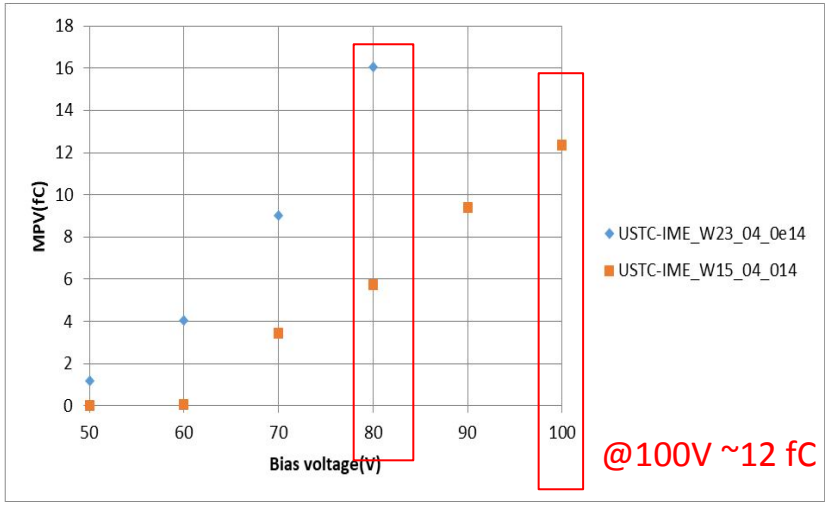

@100V ~12 fC

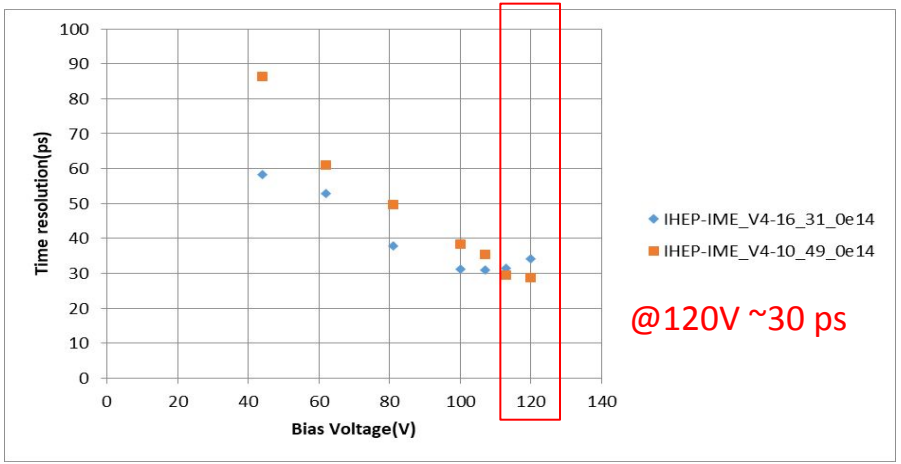

@120V ~30 ps

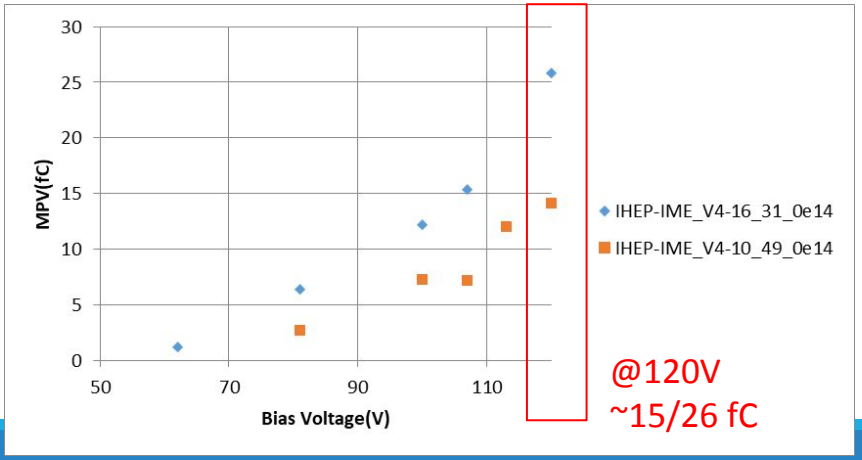

@120V
~15/26 fC

Timing results for USTC-IME_UBM_W15_04_0e14

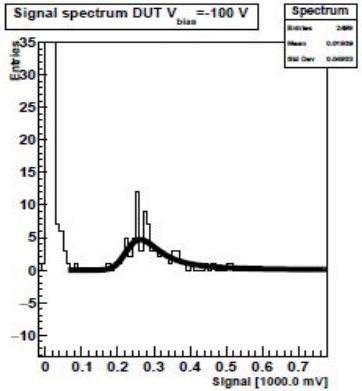

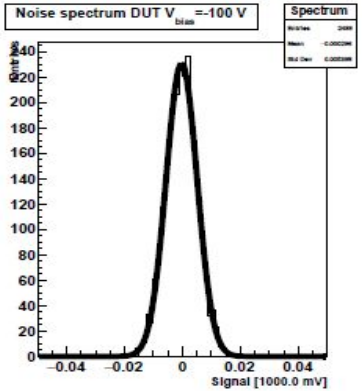

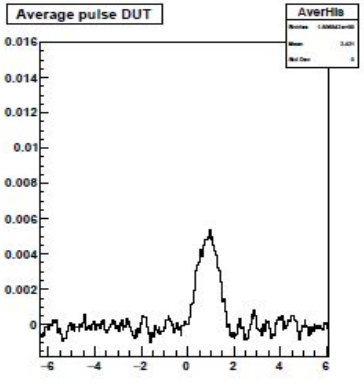

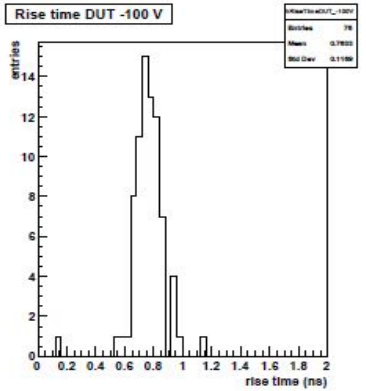

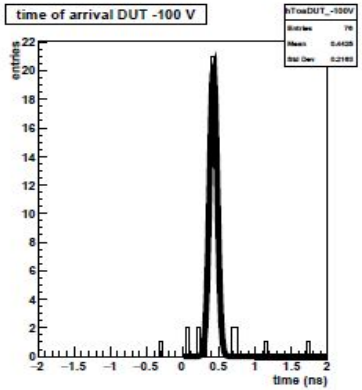

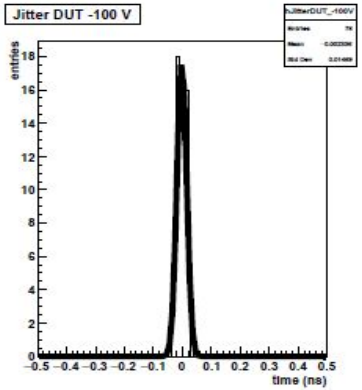

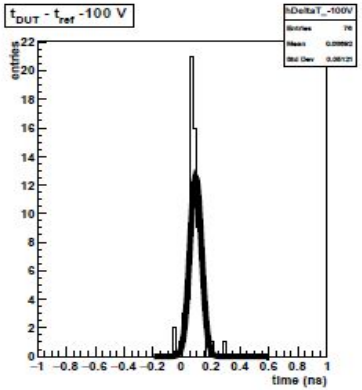

Timing results for IHEP-IME_UBM_V4_10_49_0e14

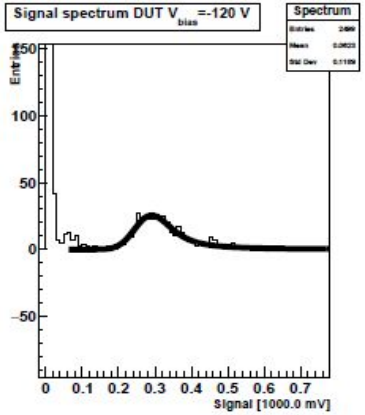

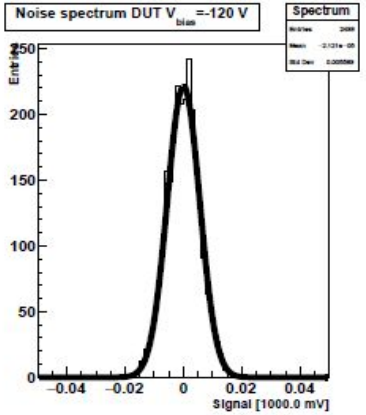

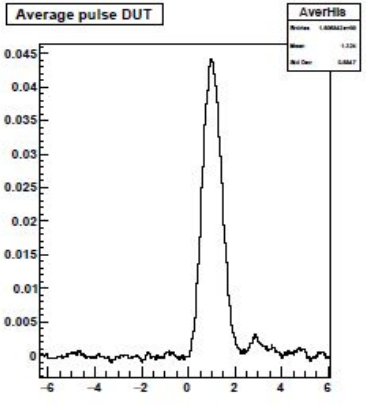

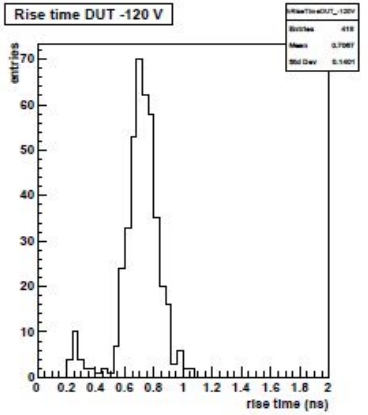

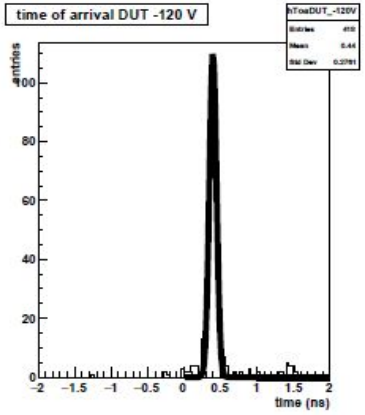

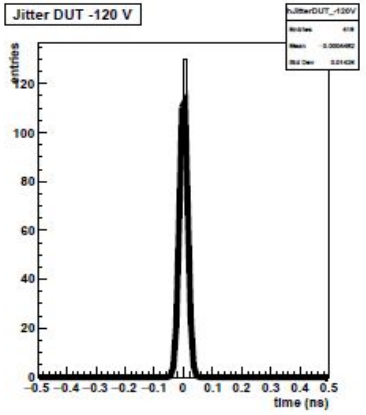

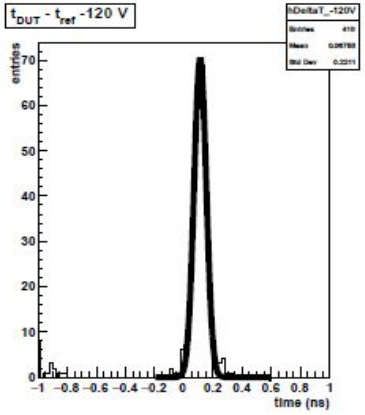

Timing/CC results for HPK HAB samples

HPK_HAB_1B+0.5HAB_0e14

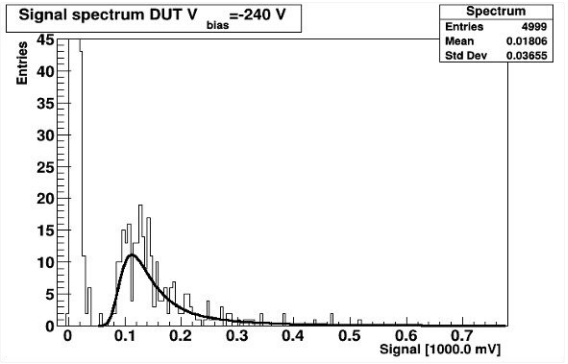

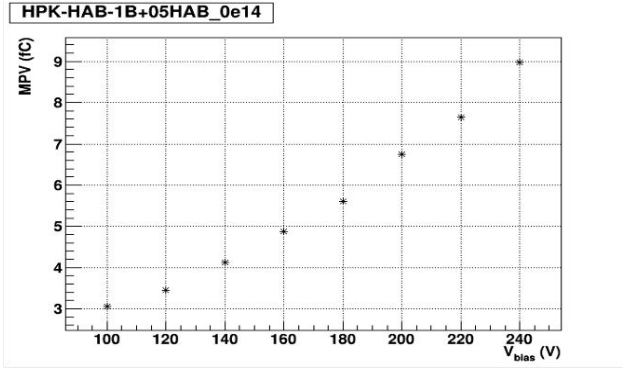

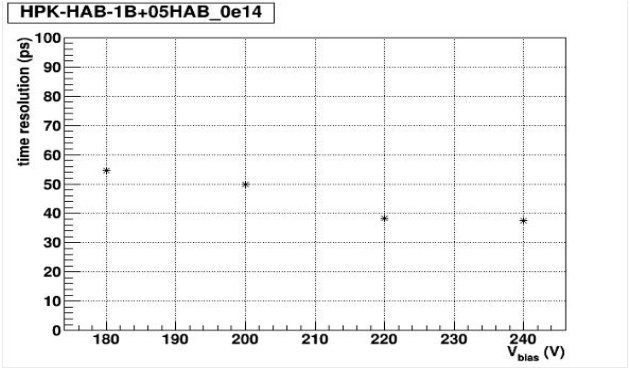

HPK_HAB_1B+1HAB_G5_15e14

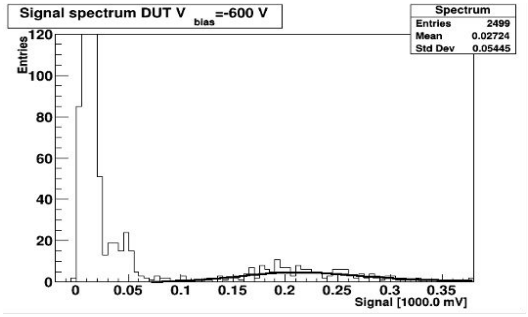

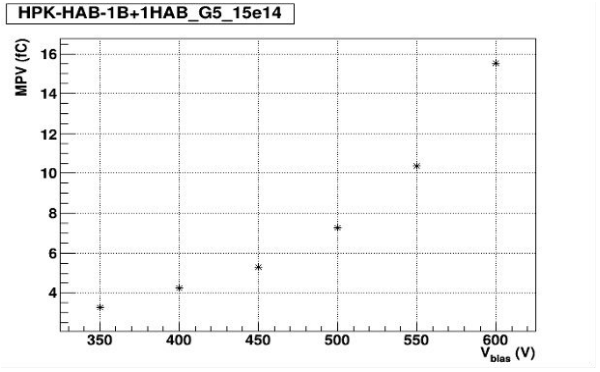

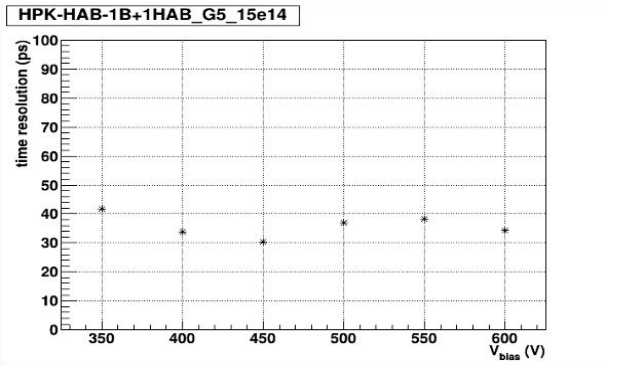

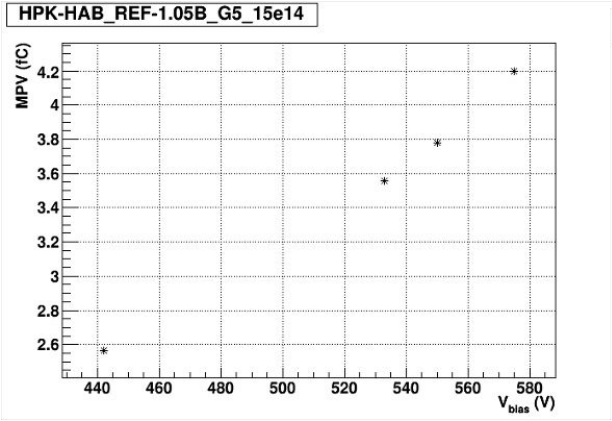
HPK-HAB_REF-1.05B_G5_15e14
MPV (fC)
4.2
4
3.8
3.6
3.4
3.2
3
2.8
2.6
440
460
480
500
520
540
560
580
V_bias (V)

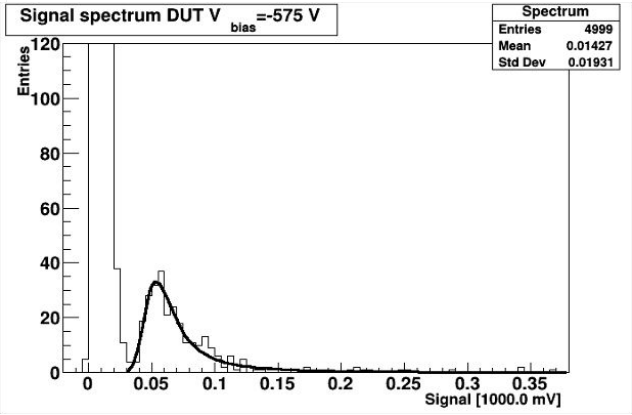
Signal spectrum DUT V bias =-575 V
Spectrum
Entries 4999
Mean 0.01427
Std Dev 0.01931
Entries
120
100
80
60
40
20
0
0
0.05
0.1
0.15
0.2
0.25
0.3
0.35
Signal [1000.0 mV]

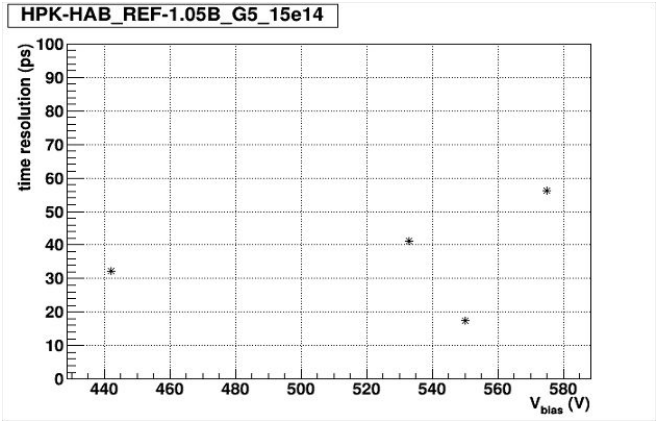
HPK-HAB_REF-1.05B_G5_15e14
time resolution (ps)
100
90
80
70
60
50
40
30
20
10
0
440
460
480
500
520
540
560
580
V_bias (V)

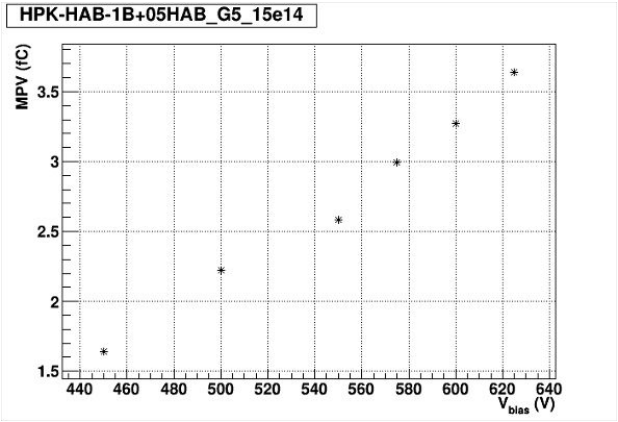
HPK-HAB-1B+05HAB_G5_15e14
MPV (fC)
3.5
3
2.5
2
1.5
440
460
480
500
520
540
560
580
600
620
640
V_bias (V)

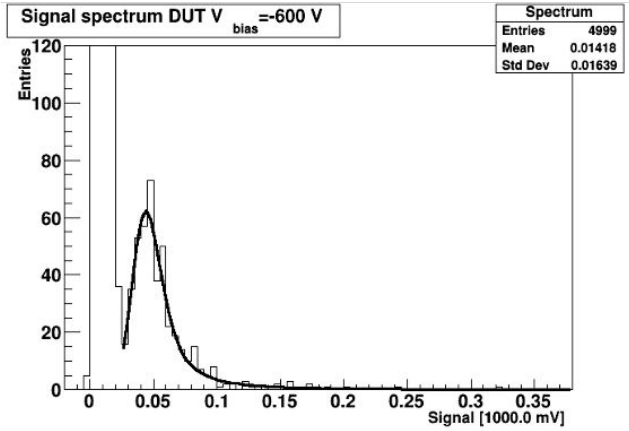
Signal spectrum DUT V bias =-600 V
Spectrum
Entries 4999
Mean 0.01418
Std Dev 0.01639
Entries
120
100
80
60
40
20
0
0
0.05
0.1
0.15
0.2
0.25
0.3
0.35
Signal [1000.0 mV]

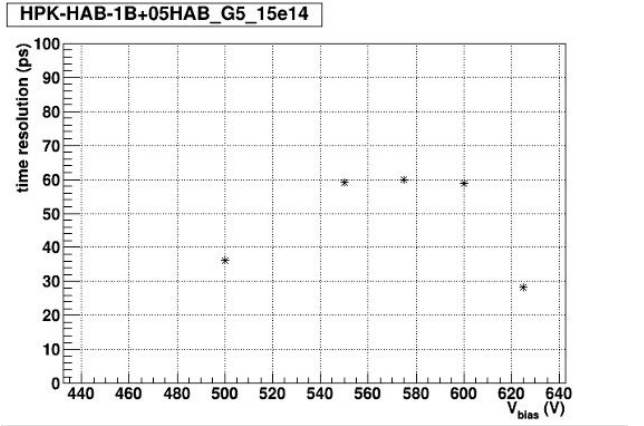
HPK-HAB-1B+05HAB_G5_15e14
time resolution (ps)
100
90
80
70
60
50
40
30
20
10
0
440
460
480
500
520
540
560
580
600
620
640
V_bias (V)

Acceptor removal constant- HPK HAB samples

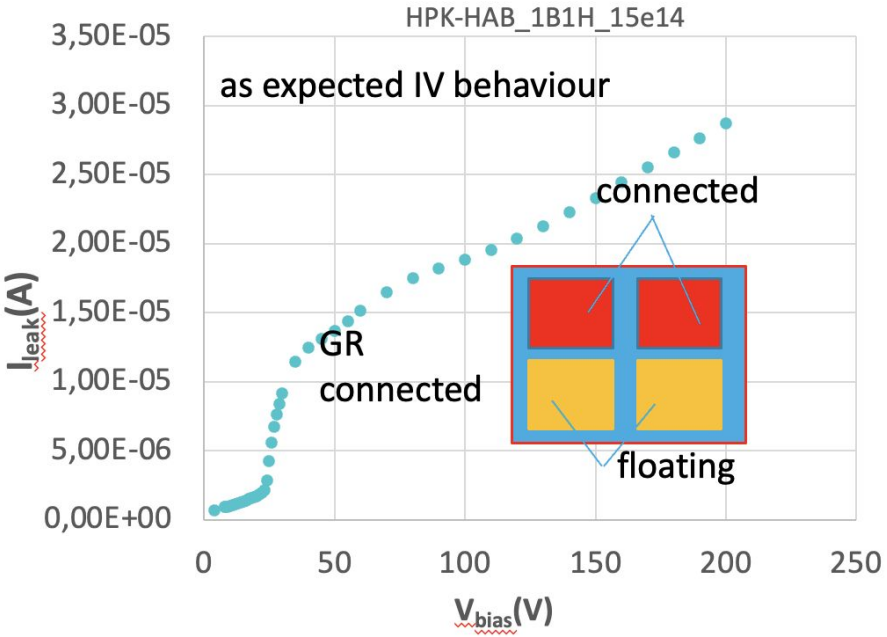

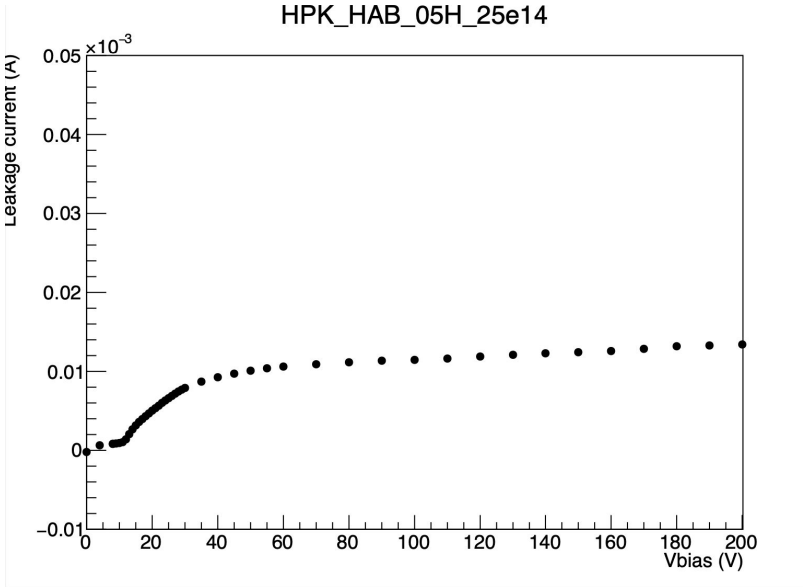

ATLAS HGTD

Timing setup and bonding for HPK samples

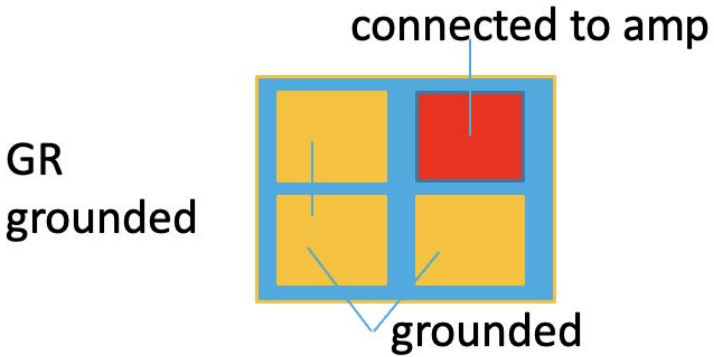

TCT/CV-IV results of UBM-ed unirradiated preproduction IHEP samples

	Fluence	CV-IV LGAD2 (next to 1x1)			TCT				
		Vgl	Vfd	Vbd (500 nA)	Vgl1	Vgl2	Vfd	Gain1 @100V	Gain2 @100V
V1R5-42	0	24.6	37	197	24.3	24.1	46.1	15	
V1R5-50	0	24.4	36	197	23.8	24.0	48.4	14.4	
V1R5-52	0	24.5	40	200	24.4	24.3	46.8	16.3	
V1R5-49	0	24.3	36	207	23.9	23.9	43.3	14.9	
V1R5-31	0	24.5	36	187	24.5	24.6	47.6	15	
Avg V1R5	**0**	**24.5**	**39.9**	**191.9**	**24.2**	**24.1**	**46.7**	**14.9**	
Std dev V1R5	**0**	**0.1**	**7.7**	**11.5**	**0.3**	**0.2**	**1.7**	**0.7**	
V4-10									
V4-10-1	0	26.2	31.6	225	26.1	26.4	52	18	18
V4-10-4	0	26.4	38.5	223	25.7	25.7	51.0	11.5	11.4
V4-10-31	0	26.5	33	210	26.0	26.0	60.0	10.5	10.2
V4-10-49	0	26	31						
V4-10-52	0	26	45	230	24.8	24.7	54.0	11.2	10.9
Avg V4-10	**0**	**26.2**	**35.8**	**222.0**	**25.7**	**25.7**	**54.3**	**12.8**	**12.6**
Stdev V4-10	**0**	**0.2**	**5.9**	**8.5**	**0.6**	**0.7**	**4.0**	**3.5**	**3.6**
V4-16									
V4-16-1	0	26.5	36	212	25.7	25.7	58.0	11.4	10.8
V4-16-4	0	26.5	27.9	199	26.3	26.5	55.9	16.5	16.5
V4-16-31	0	26.4	27.4	189	25.8	25.8	58.4	11.9	11.4
V4-16-49	0	26	31	200	25.7	25.6	57.0	12.7	12
V4-16-52	0	25.9	45	223	24.9	24.8	55.0	10.9	10.5
Avg V4-16	**0**	**26.3**	**33.5**	**204.6**	**25.7**	**25.7**	**56.9**	**12.7**	**12.2**
Stdev V4-16	**0**	**0.3**	**7.3**	**13.1**	**0.5**	**0.6**	**1.4**	**2.2**	**2.5**

TCT/CV-IV results of USTC unirradiated UBM-ed preproduction samples

	CV						TCT			
Sample	Fluence	Vbd1	Vbd2	Vfd	Vgl1	Vgl2	Vgl1-TCT	Vgl2-TCT	Gain1 at 100V	Gain2 at 100V
W15										
W15-4	0	193	183	25	24.0	24.0	24.6	24.5	10.4	10.8
W15-31	0	200	198	24.6	23.8	24.0	24.1	24.2	8.7	9.1
W15-49	0	188	168	26.3	23.3	23.8	23.9	24.3	10	9.7
average		**194**	**183**	**25.3**	**23.7**	**23.9**	**24.2**	**24.3**	**9.7**	**9.9**
stdev		**6.0**	**15.0**	**0.9**	**0.4**	**0.1**	**0.4**	**0.2**	**0.9**	**0.9**
W23										
W23-1	0	132	132	26	25.0	24.9	24.9	24.8	21.5	22.4
W23-4	0	144	153	26	24.4	24.4	24.3	24.2	19.6	18.9
W23-52	0	123.5	120	26.1	25.0	25.0	24.7	25.3	36	39
average		**133**	**135**	**26.0**	**24.8**	**24.8**	**24.6**	**24.8**	**25.7**	**26.8**
stdev		**10.3**	**16.7**	**0.1**	**0.3**	**0.3**	**0.3**	**0.6**	**9.0**	**10.7**

Measured wafers	Fluences (neq/cm^2)	V_{gl}(V)	Gain @ 100V
IHEP-IME			
W1	0.00E+00	23.00	13.30
	8.00E+14	20.50	5.90
	1.50E+15	19.00	4.20
	2.50E+15	17.60	3.40
W4	8.00E+14	20.60	5.85
	1.50E+15	19.25	3.75
W2	0.00E+00	23.43	13.24
	3.00E+15	16.30	3.10
	3.50E+15	15.80	3.20
W3	0.00E+00	24.00	19.55
	3.00E+15	16.40	3.20
	3.50E+15	15.80	2.60
USTC			
Measured wafers	Fluences (neq/cm^2)	V_{gl}(V)	Gain @ 100V
W24	8.00E+14	19.30	4.80
	1.50E+15	17.50	2.95
W2	8.00E+14	20.35	4.00
	1.50E+15	16.95	2.30

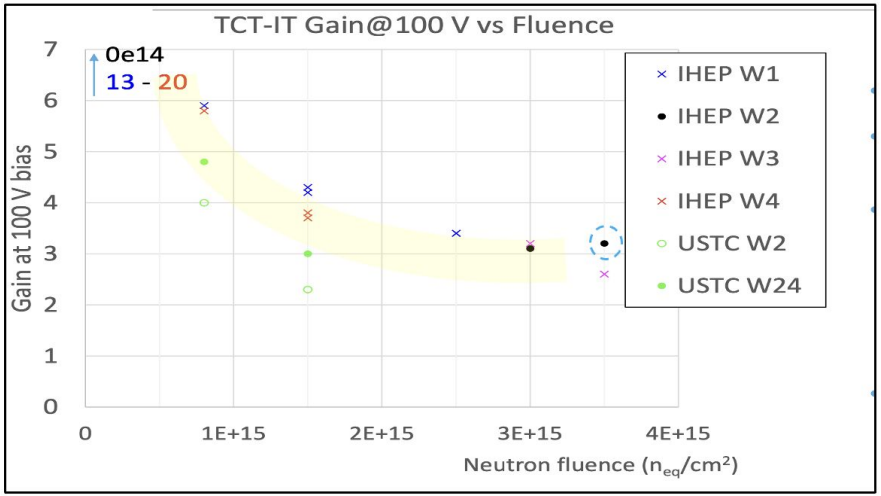

➢measured 4 wafers from IHEP-IME at fluences 0e14, 8e14, 1.5e15, 2.5e15 neq/cm^2

➢2 wafers over irradiated at 3 and 3.5e15 neq/cm^2

➢Consistent results with CV-IV measurements

➢Gain is ~20 at 0e14 neq/cm^2, after over irradiation is ~3 on average

➢gain at fixed voltage decreases with fluence as expected

TCT/CV-IV results of UBM-ed non-irradiated IHEP samples

- measured non-irradiated UBM-ed IHEP-IME samples with TCT and CV-IV
- timing measurement with Sr90 on sample V1R5_52_1x2_0e14
- Irradiated UBM-ed samples (15e14 neq/cm^2) are expected to be measured soon (already irradiated and in the fridge)
- measured V_{bd} at 500 nA
- TCT results compatible with CV-IV – slightly smaller for TCT (~0.5V)

	Fluence	CV-IV			TCT			Gain@100V
V1R5 (W5)		Vgl	Vfd	Vbd (500 nA)	Vgl1	Vgl2	Vfd	
18	0	24.7	57	180	24.7	24.1	47.8	14
22	0	24.3	37	175	24	24	47	14.7
42	0	24.6	37	197	24.3	24.1	46.1	15
50	0	24.4	36	197	23.8	24	48.4	14.4
52	0	24.5	40	200	24.4	24.3	46.8	16.3
49	0	24.3	36	207	23.9	23.9	43.3	14.9
31	0	24.5	36	187	24.5	24.6	47.6	15

Quality check- TCT: IHEP-IME V1R3_18_3.5e15

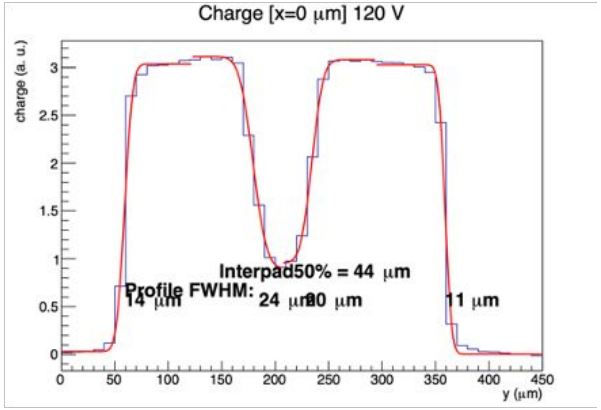

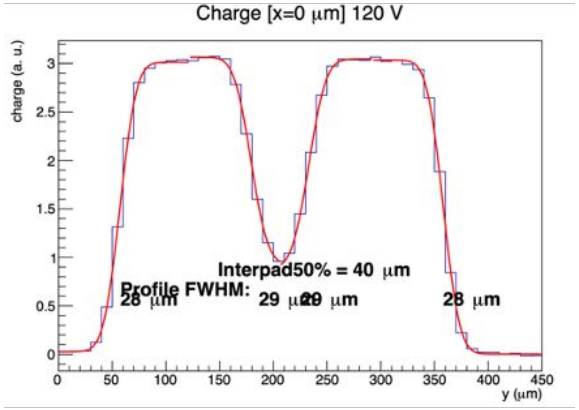

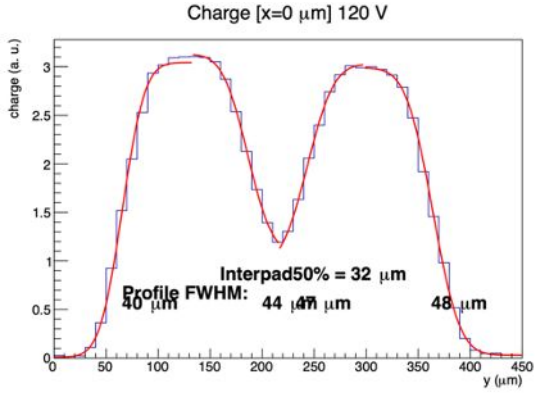

- Data quality monitoring has been implemented in the TCT analysis
- It's important to have good focus due to gain changes that happen because of bad/good focus (shown on the plot) for 11, 28 and 48 um focus

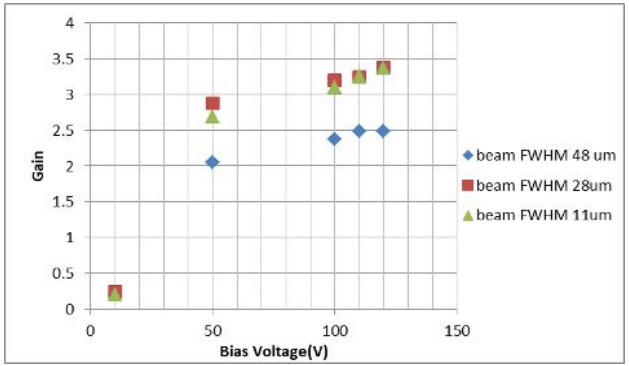

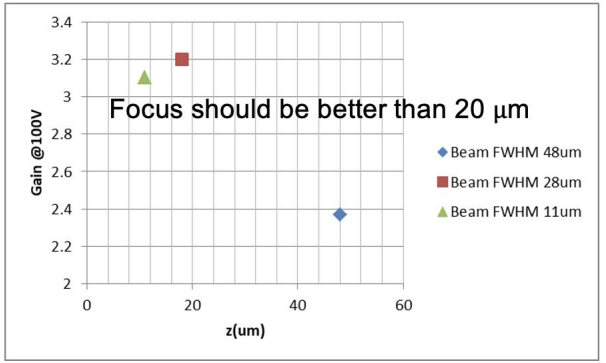

ATLAS HGTD

TCT and timing results for UBM-ed sample W5-52 0e14

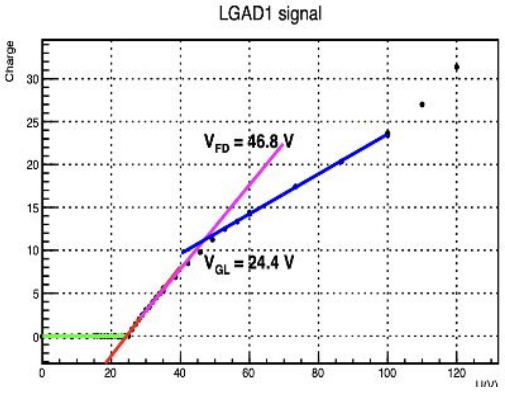

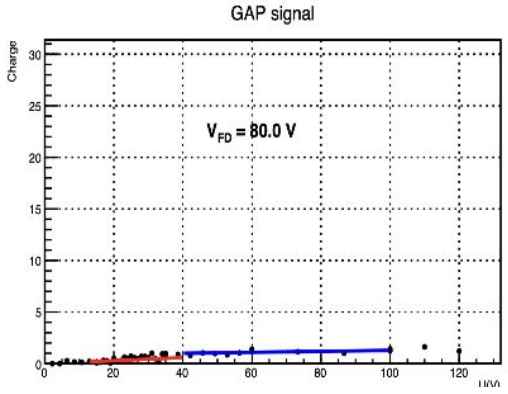

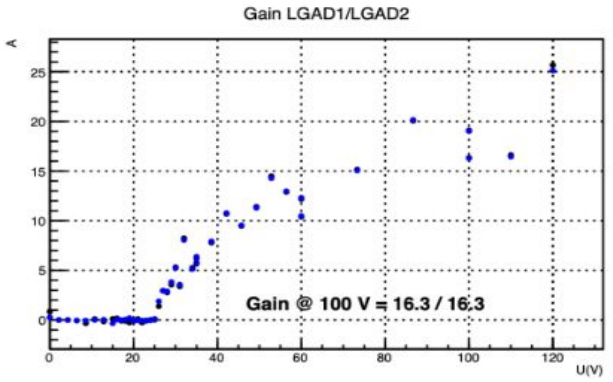

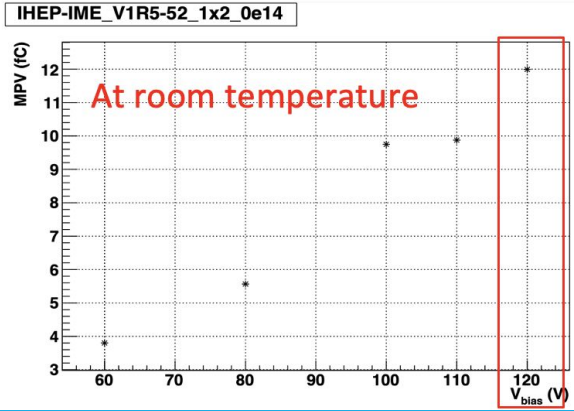

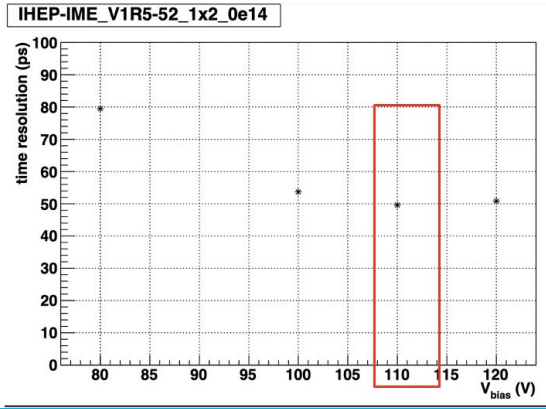

➢Unirradiated UBM sample shows good results (gain is 16.3 @100V, Vgl=24.4)

➢Time resolution is below 50 ps @110 V

➢Collected charge @120 ~12fC

➢Temperature dependence timing measurement

Timing performance of LGAD at different temperature: UBM-ed V1R5-52-0e14

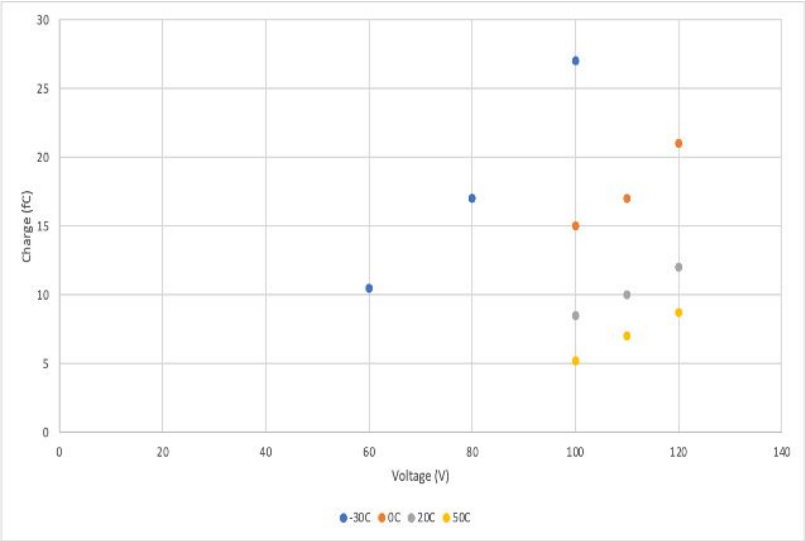

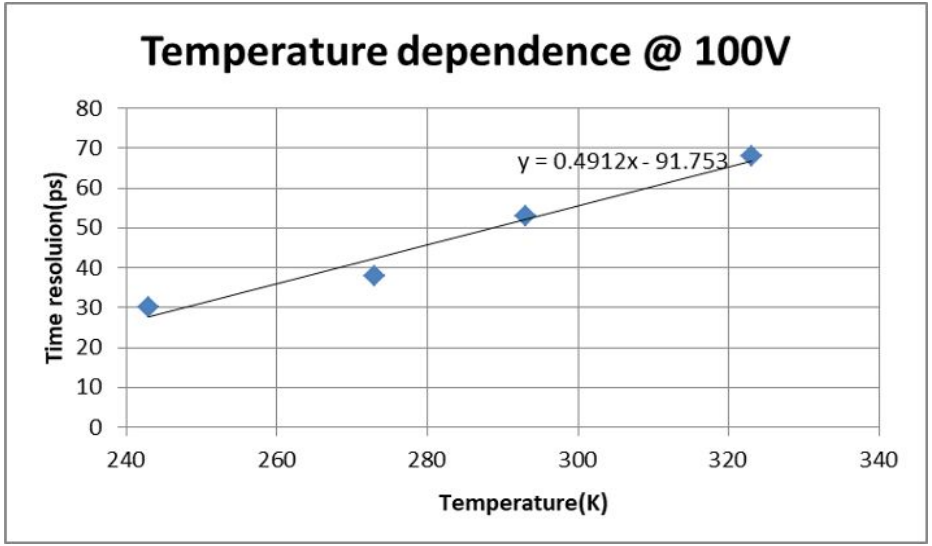

- Collected charge degraded at higher temperatures
- At 100 V charge reaches 27 fC at -30 ℃
- At 50 ℃ collected charge is 5fC
- At 100 V time resolution for 50 ℃ is ~65 ps, at -30 ℃ it's ~30 ps
- Vbd increases with temperature

2D TCT scans

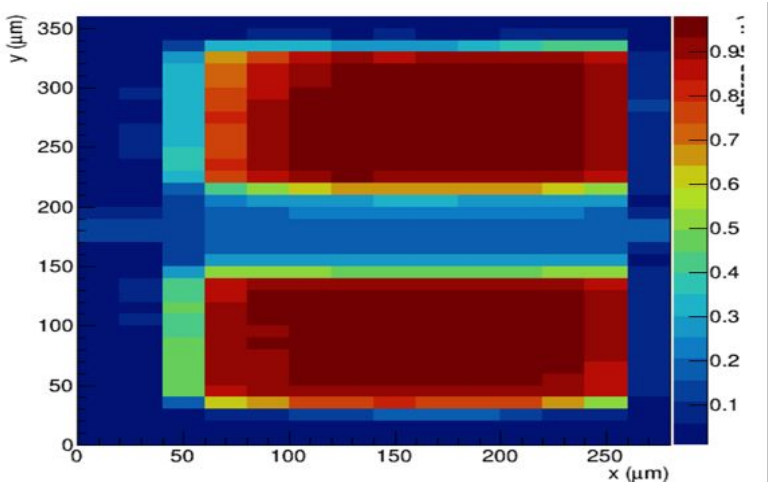

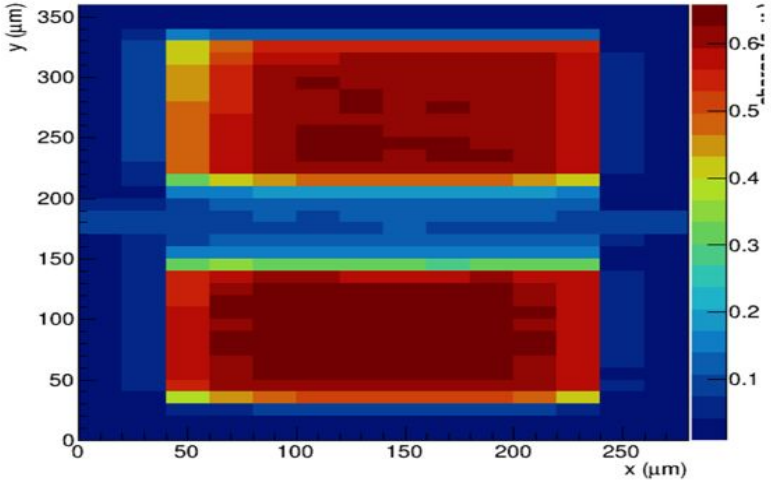

- used sample: V2-#I2-14_1.5E14
- minimal mechanical changes
- displacement of around 20 µm
- conclusion: reliable temperature scans

Temperature dependence of gain and timing

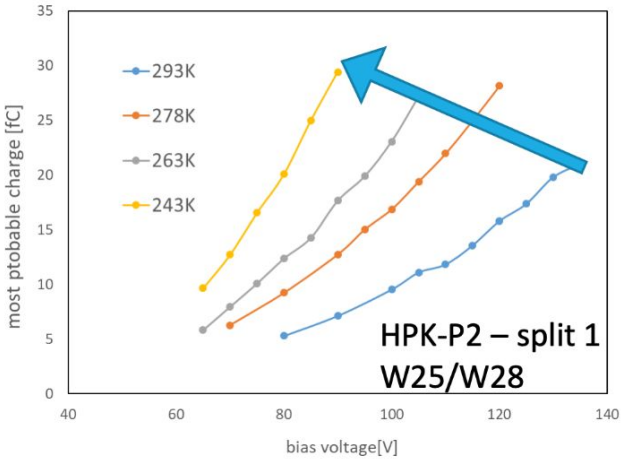

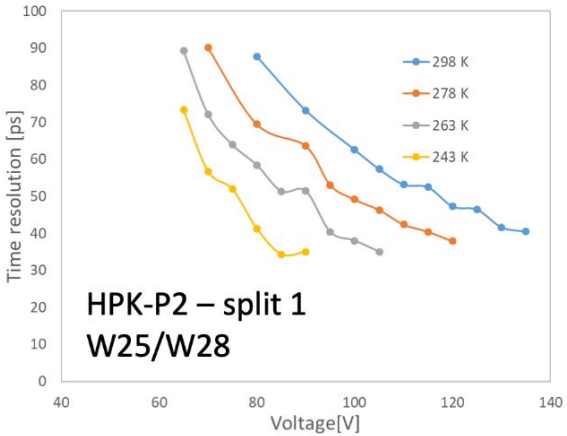

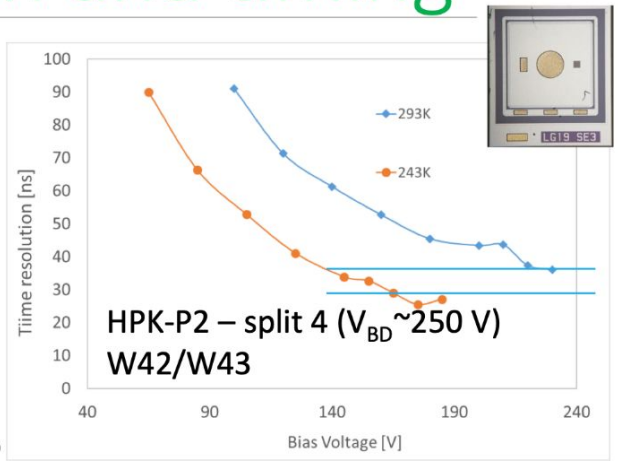

- Impact ionization – gain mechanism is a strong function of temperature – so breakdown voltages at -30°C are much lower than at room temperature (50-80 V) – variation of temperature over the sensors in experiments has to be well controlled in narrow window of few degrees
- If electric fields are high enough to provide drift velocities close to saturation lower temperature decrease the drift time and by that improves the time resolution.

TCT gain results at 100V vs T (°C)

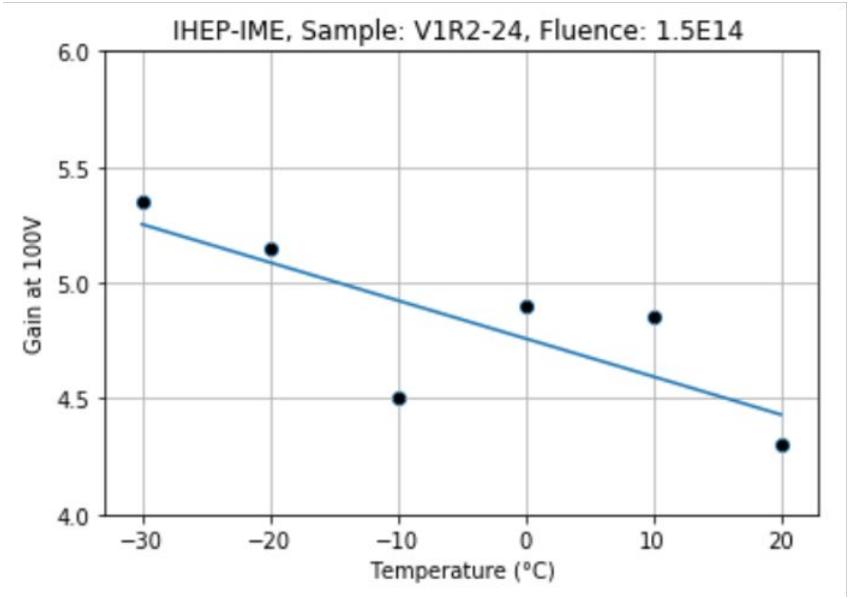

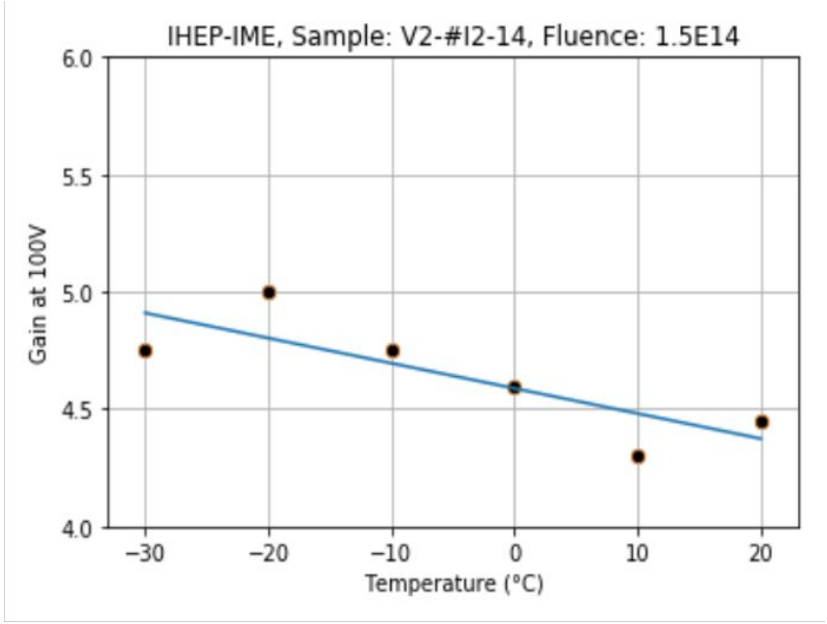

Sensor types studies – few examples

SINGLES

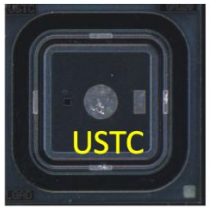

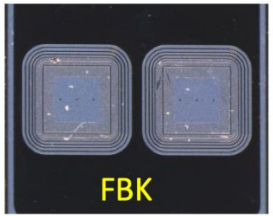

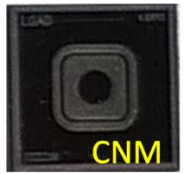

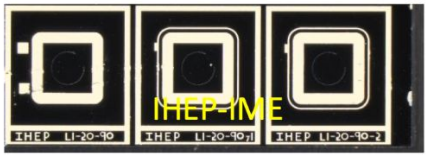

2x2 array

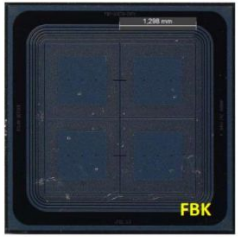

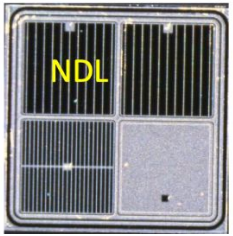

5x5 array

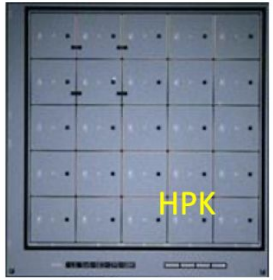

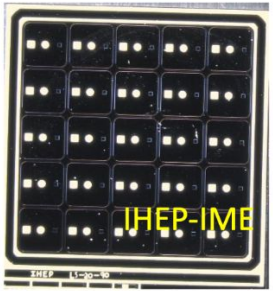

Full size sensors 15x15(16x16) arrays

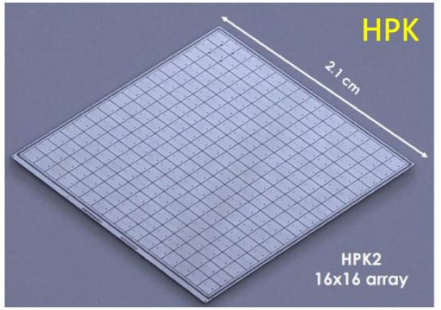

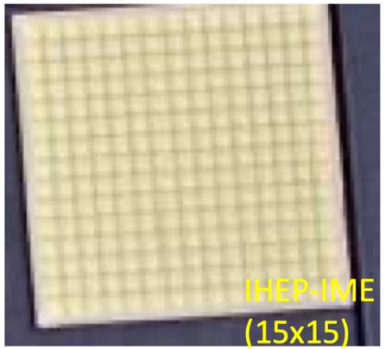

Measuring the performance of the detectors

modified plot from N. Cartiglia

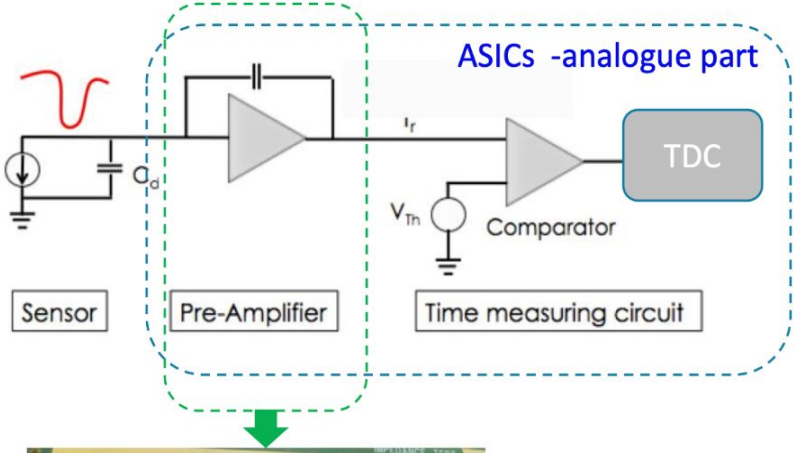

Beta scope – used for ^{90}Sr and in test beams

Timing and Charge measurements

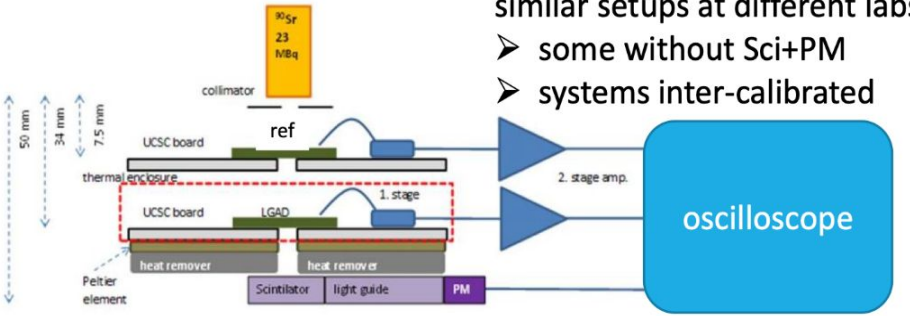

similar setups at different labs

- some without Sci+PM
- systems inter-calibrated

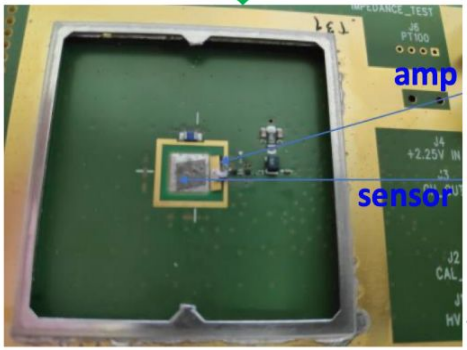

UCSC boards is mostly used

- transimpedance amp (470Ω), Si-Ge
- wide bandwidth 3 GHz
- 1 and 4 Ch. versions

Less constraints with respect to the ASICs – exploring the limits of the sensors.

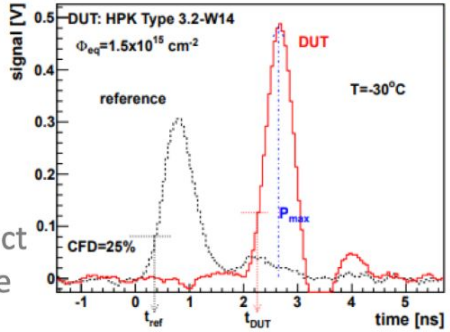

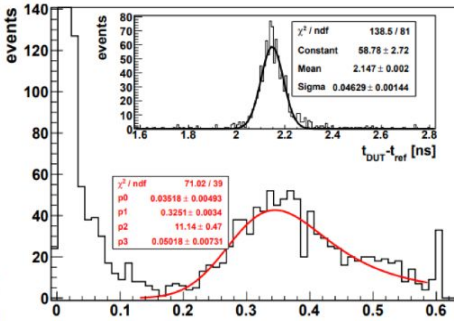

Introduction to Silicon sensors

- Innermost layers of high energy physics accelerator-based experiments require:
  - Position resolution, rate capability, compactness, low material budget, radiation hardness
  - Chosen technology: silicon pixel sensors

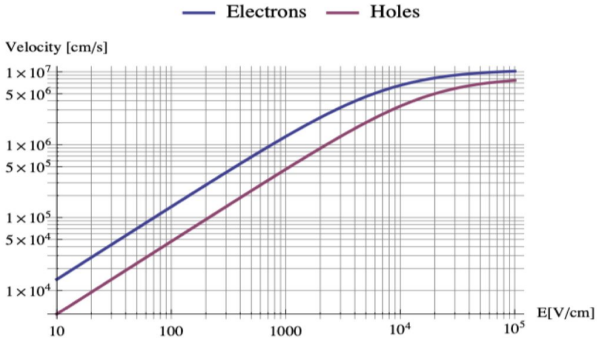

At high electric fields, the drift-velocity saturates around 107 cm/s = 0.1µm/ps for both, electrons and holes

- Doping in Silicon:
  - n-type Silicon-> electrons are majority carriers
  - p-type Silicon-> holes are majority carriers
- p-n junction under reverse V_{bias}
  - Depleted zone-> widens

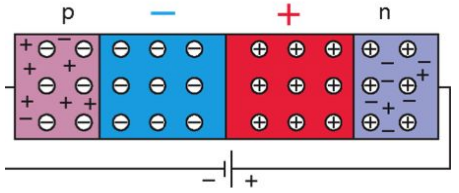

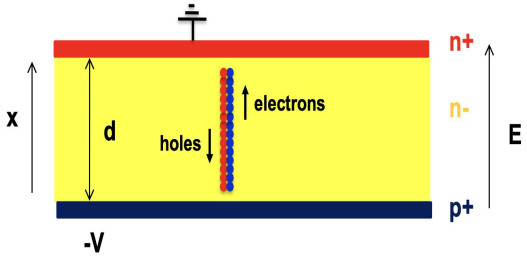

In a 50 um sensor at very high voltage electrons and holes take around 500 ps to move through the sensor.

Pixel module

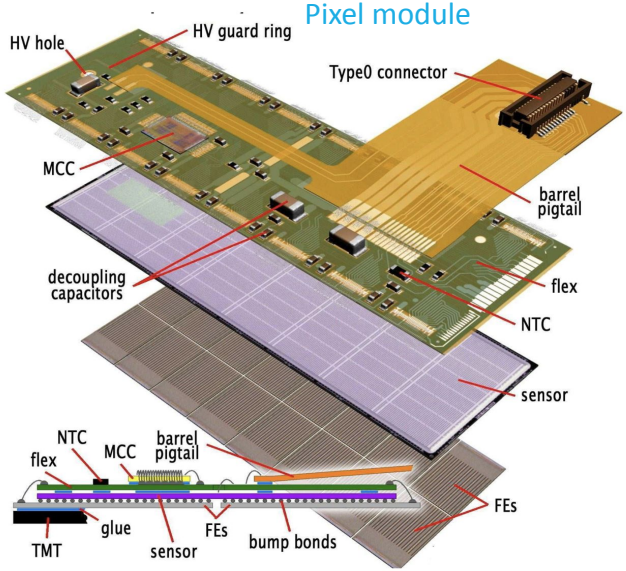

- sensor is bump-bonded to integrated circuit-> Application-Specific Integrated Circuit (ASIC)

3D Irradiated - 50×50 μm²

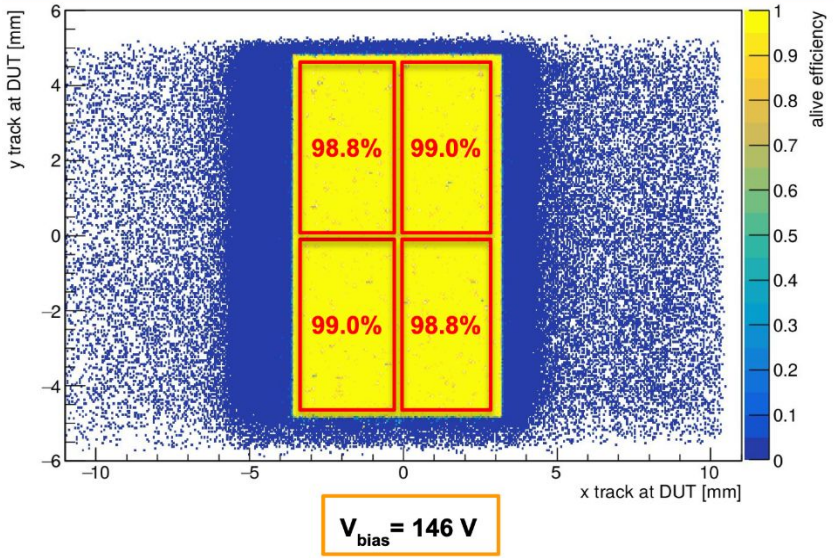

V_{bias} = 146 V

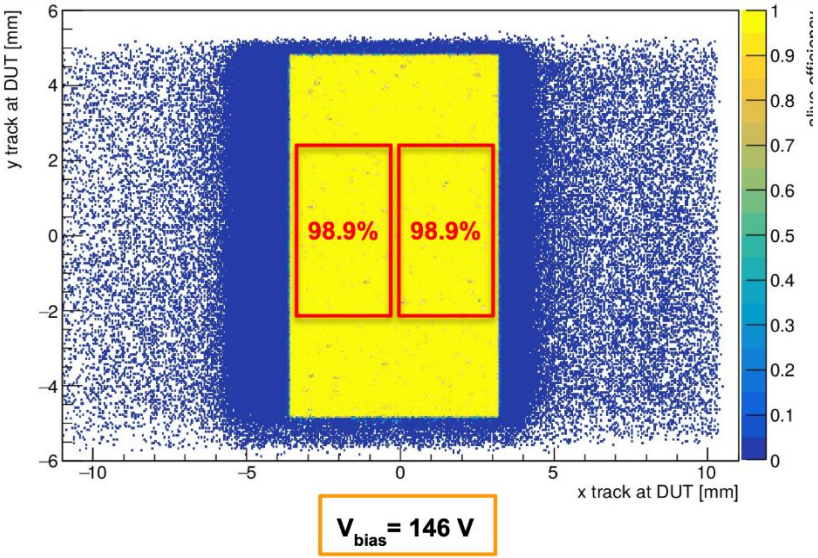

V_{bias} = 146 V

- Efficiency evaluated on smaller zones (red boxes)
- No significant drops in efficiency have been observed in the irradiation spot
- Efficiency is uniform across the sensor, at least at high V_{bias}